Measuring Transversity from Pion-Pairs using a Longitudinally Polarized Target

A thesis submitted in partial fulfillment of the requirement
for the degree of Bachelor of Science with Honors in Physics
from the College of William and Mary in Virginia,

by

Nicholas Ian Walsh

Accepted for _____
(Honors)

_____
Dr. Keith Griffioen, Advisor

_____
Dr. Todd Averett

_____
Dr. Gina Hoatson

_____
Dr. Timothy Killingback

Williamsburg, Virginia
May 2007

Acknowledgments

I would like to thank Dr. Griffioen for patiently guiding me through this project. I also want to thank my family and friends for all their support they have given me.

Abstract

In the search for the origin of the proton spin, quark transversity is of great interest but is still poorly measured. Transversity is the probability of finding a transversely polarized quark in a target polarized transverse to the incident electron beam. A single spin asymmetry measured from a semi-inclusive pion-pair electroproduction process is used as a probe of transversity. The asymmetry, measured from a longitudinally polarized target, is a function of the azimuthal angle $\phi_{R\perp}$, which is the angle between the scattering plane and the 2-pion plane. The $\sin\phi_{R\perp}$ moment of the asymmetry is proportional to $h_1 H_1^{\sphericalangle}$, where h_1 is the transversity distribution and $H_1^{\sphericalangle}$ is the 2-pion fragmentation function. The $\sin\phi_{R\perp}$ moment is typically less than 0.002 in magnitude and negative. The data were taken from the EG1b run period from CLAS in Hall B of Jefferson Lab with a 5.7 GeV electron beam.

Contents

List of Figures

List of Tables

1 Introduction

1.1 Nucleon Structure

At the smallest scale, matter is composed of fundamental particles. These include leptons (electrons, neutrinos, etc.), quarks, and the force carriers (photons, gluons, etc.). Each is considered to be a point-like particle. Quarks form quantum mechanical bound states as pairs or triplets, collectively called hadrons. The nucleon (a neutron or proton) is the lowest energy three-quark hadron state, and is the building block of the atom's nucleus.

In 1988, an experiment was performed to measure the spin contribution of the quarks relative to the total proton spin [1]. Surprisingly, the quarks contributed very little to the total proton spin. This has been called the spin crisis. A decade of measurements have confirmed that the quarks are responsible for only 20% of the proton's spin [2, 3]. The only other possible sources of proton spin are the gluon spin or the orbital angular momentum. Since the spin crisis, much has been learned about the other spin structure functions in the proton but very little is known about transversity. Transversity is the distribution of transversely polarized quarks in a transversely polarized target. Transverse refers to the perpendicular angle between the incident particle and the target spin directions. Other polarizations include the unpolarized nucleon and longitudinally polarized target, as shown in Fig. 1 [4].

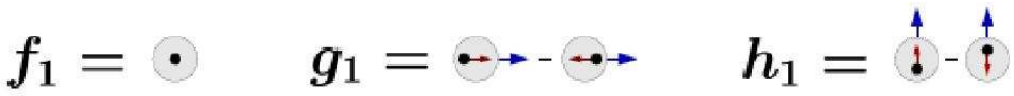

Figure 1: Three primary nucleon structure functions. All directions are relative to an incident beam coming horizontally toward the target. The arrow outside the circle corresponds to the spin direction of the nucleon, whereas the arrow inside the circle corresponds to the quark spin direction. Here f_1 is the distribution of unpolarized quarks in an unpolarized nucleon. The function g_1 is the difference in distributions of quarks polarized longitudinally along and opposite the nucleon spin. Similarly, h_1 is the difference in distributions along and opposite the nucleon spin for transversely polarized quarks [5].

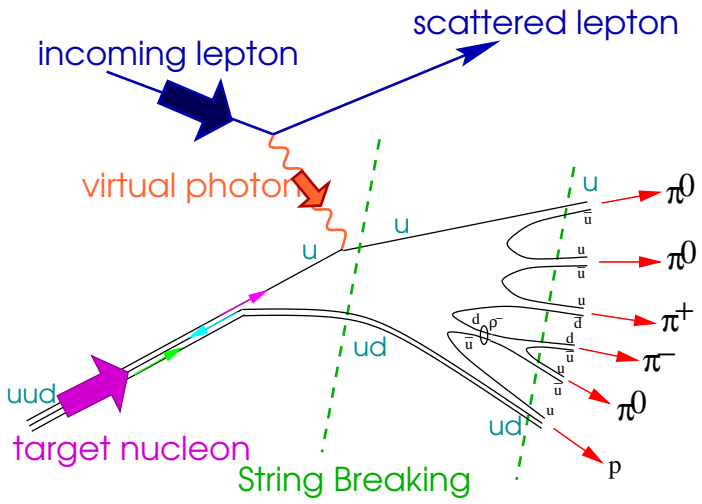

Figure 2: Pion production in deep inelastic scattering from a proton. The incident electron scatters via virtual photon exchange with a quark in the nucleon. As the struck quark moves away from the spectator quarks, the strong force creates a string of quark-antiquark pairs. The string breaks into hadrons states such as a π^+, π^- and a nucleon [6].

1.2 Scattering Process

Measuring transversity requires colliding a high energy electron with a polarized proton and observing a single spin asymmetry. A quark struck by a high energy electron does not have time to interact with the other quarks in the nucleon at the moment of interaction. With the sudden increase in momentum, the struck quark pulls away from the two spectator quarks. This creates a strong force field which breaks into a string of quark-antiquark pairs. The quarks separate and form various hadrons states. Figure 2 shows an electron scattering via virtual photon from one of the quarks in a proton. The creation of quarks and antiquarks can vary greatly and what is shown is only one possibility.

We measure the semi-inclusive reaction $e^- + p \rightarrow e^- + \pi^+ + \pi^- + X$. Here an electron ($e^-$), scatters off a proton (p), and creates a pion-pair ($\pi^+\pi^-$). Whatever other hadrons are created are left unmeasured and included in X. The proton and neutron have three quarks and spin-$\frac{1}{2}$, but the pion, short for pi-meson, has two quarks and spin-0. As shown in Table 1, the π^+ and π^- are made of a simple quark-

antiquark combination of up (u), down (d), anti-up ($\bar{u}$), or anti-down ($\bar{d}$) quarks. The π^0 is a linear superposition of states. The u and d quarks are the two lightest quarks, and similarly, pions are the lightest meson with a mass of 139 MeV/c^2. Thus, pions are the mostly likely particles emitted in *ep* reactions.

Pion	Charge	Quark Combination
π^+	+1	$\bar{d}u$
π^0	0	$(\bar{d}d + \bar{u}u)/\sqrt{2}$
π^-	-1	$\bar{u}d$

Table 1: Pion types and quark constituents . The pion is made of a combination of an up (u) or down (d) quark and an anti-up ($\bar{u}$) or anti-down ($\bar{d}$) antiquark. The π^0 is a linear superposition of two states.

1.3 Experimental Setup

The measurement for transversity requires a powerful electron accelerator, a polarized target, and a large acceptance detection system capable of simultaneously measuring the scattered electron and a pair of pions. The Jefferson Lab (JLab) electron beam and the Hall B CLAS spectrometer meet these requirements. The CEBAF accelerator at JLab produces a high luminosity continuous electron beam with up to 6 GeV of energy. Although our measurement requires that the incident electron be unpolarized, we sum over all beam polarization directions to cancel polarized beam effects. We can determine the electron's wavelength using De Broglie's formula, $\lambda = hc/E$ such that the 6 GeV electron beam at JLab has a resolution on the order of 0.2 fm or about 1/10 the diameter of a proton. The experiment was run at three other beam energies. This particular data set is the highest energy from two similar energies of 5.628 and 5.735 GeV. All the data used were taken between September 8, 2000 and April 20, 2001 and calibrated by the Hall B EG1b Run Group at JLab [7].

The primary target was polarized frozen ammonia ($^{15}NH_3$). The target was polarized parallel and anti-parallel with the incoming electron beam. After our cuts,

we used 264,072 events from the parallel target which had an average polarization of 77.3%, and 251,660 events from the antiparallel target which had an average polarization of 71.2%. The lower polarization for the antiparallel case is due to the limitations the magnetic field in the detector. To get only the effect of the polarized protons, we must subtract out the contribution from the largely unpolarized nitrogen nucleus. To do this, data from an unpolarized carbon target (^{12}C) was taken and by scaling the carbon to the size of nitrogen, isolating the proton events is possible.

Data were taken using the wide angular acceptance of the CLAS detector [8]. The CLAS detector has many layers of detection as depicted in Fig. 3. Nearest to the target are the drift chambers consisting of thin wires with a voltage potential that detects charged moving particles. The moving particles move through the interior gas ionizing it. The free electrons are collected at the wires where a signal is induced and measured. The chamber is placed in a magnetic field, such that any particle moving perpendicular to the field will feel a force according to the Lorentz formula, $\vec{F} = q(\vec{E} + \vec{v} \times \vec{B})$. The direction of $\vec{B}$ is along the beam direction, so any particle moving scattered away from the incident beam will feel this force. The Cherenkov counter uses a material in which a charged particle can travel faster than the speed of light in that medium. As a result, a shower of photons is created in an electromagnetic shockwave, and detected with photo-detectors. The time-of-flight of a particle is measured further away from the target with scintillating material. On the outermost shell is the calorimeter, layered with lead and scintillators which measures an electron's or photon's energy. Together, the calorimeter and Cherenkov detectors are able to distinguish electrons from pions.

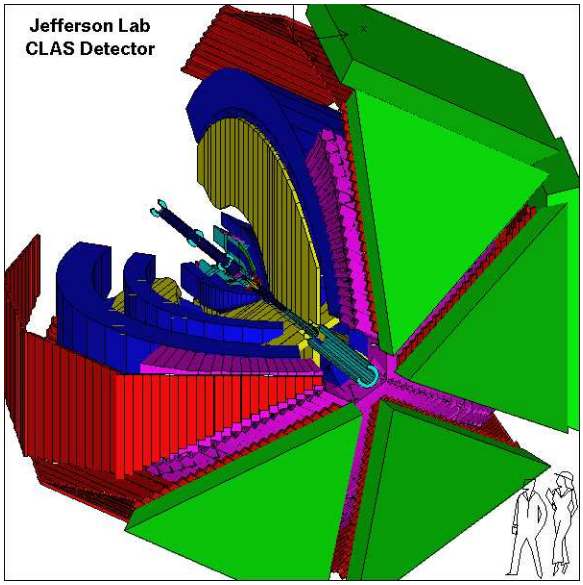

Figure 3: Schematic of the CLAS detector in Hall B. The innermost line is the incoming electron beam. Surrounding the target are the cryostats (yellow) of the superconducting magnets. The drift chambers (blue) measure the ionization track of a charged particle that curls in the magnetic field. Around that are the Cherenkov counters (purple) that produce an electromagnetic shock wave only for particle that travel faster than the speed of light in the gas. The time-of-flight measurements are made by the scintillators (red). The outermost layer is the calorimeter (green) which measures particle energy using layers of lead and plastic scintillators. The Chernkov detector and the calorimeters together are used to distinguish electron from pions.

2 Kinematics

2.1 Scattering Kinematics

Each event is described knowing the beam energy and the final momentum of the electron and two pions. The incoming electron beam is chosen to be traveling in the positive $\hat{z}$-direction. The energy can be written as

$$E^2 = mc^2 + (pc^2)^2, \tag{1}$$

for energy E in GeV, mass m in GeV/c^2, and momentum p in GeV/c. By setting $c = 1$ and expressing mass and momentum in units of GeV, the notation becomes much simpler. The notation of four vectors, $E_\mu = (E, \vec{p})$, is the standard for relativistic

mechanics. The incident electron can be written as

$$k_\mu = (k, 0, 0, k), \tag{2}$$

where k is the incoming electron beam energy and at relativistic speeds, the total energy $E = \sqrt{m^2 + p^2} \approx p$. The scattered electron's four-momentum is

$$k'_\mu = (k', k' \sin\theta \cos\phi, k' \sin\theta \sin\phi, k' \cos\theta), \tag{3}$$

where (θ, ϕ) are the polar and azimuthal angles of scattering defined from the direction of the incident electron in the lab frame.

The difference between the incident and scattered four-momenta defines the four-momentum energy transfer q_μ. The laws of energy and momentum conservation require that $k_\mu = k'_\mu + q_\mu$. The four-momentum q is defined as

$$q_\mu = k_\mu - k'_\mu = (\nu, \vec{q}). \tag{4}$$

This is the four-momentum describing the virtual photon exchanged between the electron and the proton target.

The scattering process, shown in Fig. 4, produces two pions after an incident electron scatters off a polarized target. The momentum of the pions are measured in the lab frame as

$$\begin{aligned} \vec{P}_1 &= (P_{1x}, P_{1y}, P_{1z}) \\ \vec{P}_2 &= (P_{2x}, P_{2y}, P_{2z}). \end{aligned} \tag{5}$$

For this analysis, the π^+ momentum is denoted by $\vec{P}_1$, and the π^- momentum by $\vec{P}_2$. The sum of the pion vectors is defined as

$$\vec{P}_h = \vec{P}_1 + \vec{P}_2. \tag{6}$$

Additionally, the energy of a pion may be computed using Eq. 1 and the four-

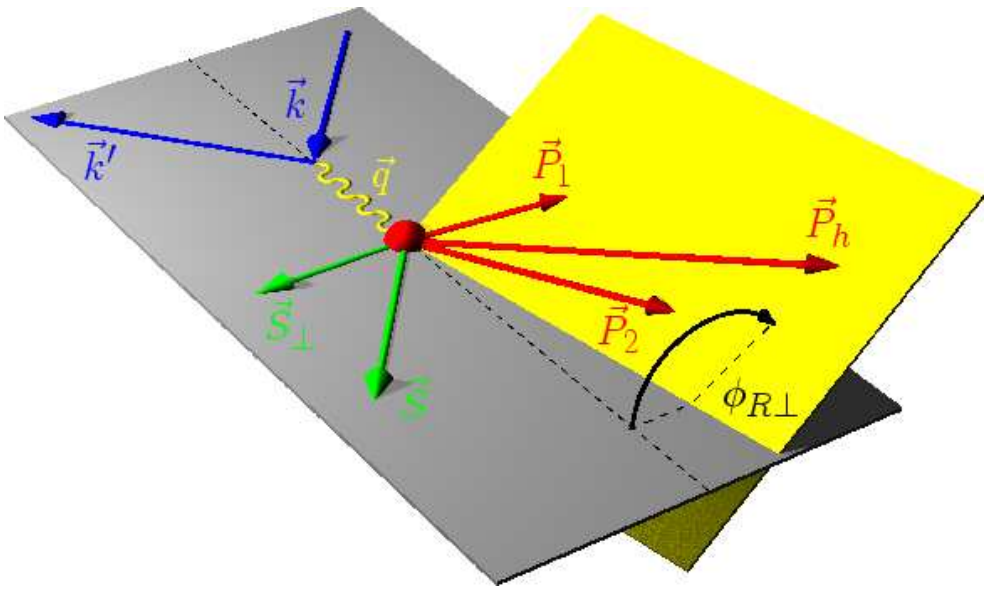

Figure 4: Pion-pair production in lepton scattering from a polarized target. An incident lepton, $\vec{k}$, scatters with momentum $\vec{k'}$ off a fixed target by exchange of a virtual photon $\vec{q}$. The target is polarized longitudinally such that $\vec{S}$ is parallel to the direction of $\vec{k}$. The transverse component of the polarization $S_\perp$ is the component perpendicular to the virtual photon. The angle, $\phi_{R\perp}$, is measured between the plane defined by the scattered electron and the plane defined by the pion-pair, $\vec{P}_1, \vec{P}_2$. P_h is the sum of the two pions [6].

momentum may be written as

$$\begin{aligned} P_{1\mu} &= (E_1, \vec{P}_1) \\ P_{2\mu} &= (E_2, \vec{P}_2). \end{aligned} \tag{7}$$

The sum is similarly defined as

$$P_{h\mu} = P_{1\mu} + P_{1\mu}. \tag{8}$$

Using the Trento conventions [9], R is defined as

$$\vec{R} = \frac{(\vec{P}_1 - \vec{P}_2)}{2}. \tag{9}$$

The vector perpendicular to $\vec{P}_h$ in the plane defined by $\vec{P}_1$ and $\vec{P}_2$ is defined to be

$$\vec{R_T} = \vec{R} - (\vec{R} \cdot \hat{P}_h)\hat{P}_h, \tag{10}$$

where the unit vector is

$$\hat{P}_h = \frac{\vec{P}_h}{\sqrt{|\vec{P}_h|^2}}. \tag{11}$$

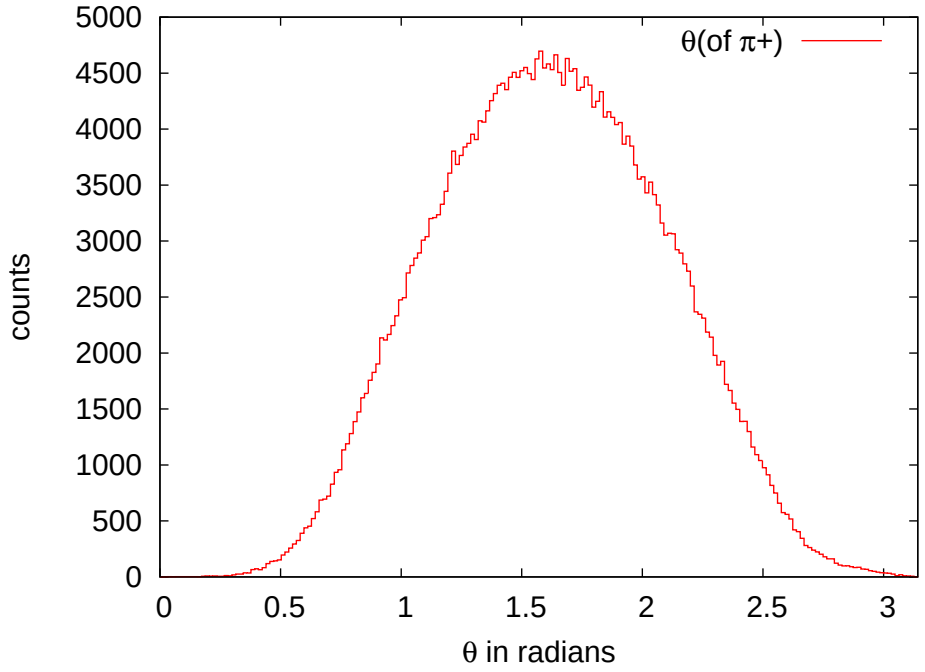

Figure 5: Histogram of Θ^{cm} for π^+ in pair center-of-mass frame. The reference angle ($\Theta^{cm} = 0$) corresponds to the direction of $\vec{P}_h$. The π^- angle is exactly $\Theta^{cm(-)} = \pi - \Theta^{cm}$. Thus, the two pions always scatter in opposite directions in the pair pair center of mass frame.

Finally, the azimuthal angle measured between the plane defined by the scattered electron and the plane defined by the pion-pair is calculated as

$$\phi_{R\perp} = \frac{(\vec{q}\times\vec{k})\cdot\vec{R}_T}{|(\vec{q}\times\vec{k})\cdot\vec{R}_T|}\arccos\frac{(\vec{q}\times\vec{k})\cdot(\vec{q}\times\vec{R}_T)}{|(\vec{q}\times\vec{k})|\cdot|(\vec{q}\times\vec{R}_T)|}. \tag{12}$$

The angle is also specified to be perpendicular to the virtual photon.

The polar angle Θ^{cm} is the angle of the π^+ emission with respect to the direction the pair momentum evaluated in the pion-pair center-of-mass frame. It can be calculated from experimental data as

$$\Theta^{cm} = \arccos\left[\frac{\vec{R}^{cm}\cdot\vec{P}_h}{|\vec{R}^{cm}|\cdot|\vec{P}_h|}\right]. \tag{13}$$

In Fig. 5, the distribution of Θ^{cm} shows most scattering occurs at 90° where the π^+ momentum has the same magnitude of the π^-. In the pair center-of-mass frame the distribution of the π^- is given by $\Theta^{cm(-)} = \pi - \Theta^{cm}$. To get to the center-of-mass frame a Lorentz invariant boost redefines the coordinate system in the direction of of

the pion pair $\vec{P}_h$

In the pion-pair center-of-mass the momentum of the pair is 0. Using the relativistic form of Eq. 1, $E = \gamma M_h$, the relativistic factor γ is defined in terms of the pion-pair by

$$\gamma = \frac{E}{M_h} = \frac{E_1 + E_2}{\sqrt{P_{h\mu} \cdot P_h^{\mu}}}. \tag{14}$$

The mass M_h is the mass of the pion-pair. With $\beta = \sqrt{1 - 1/\gamma^2}$ the four-momentum components of the pions in the pion-pair rest frame are given by

$$E_i^{cm} = \gamma(E_i - \beta \vec{P}_{iz}), \tag{15}$$

$$\vec{P}_{ix}^{cm} = \vec{P}_{ix}, \tag{16}$$

$$\vec{P}_{iy}^{cm} = \vec{P}_{iy}, \tag{17}$$

$$\vec{P}_{iz}^{cm} = \gamma(\vec{P}_{iz} - \beta E_i), \tag{18}$$

where $i = 1, 2$, and only the $\hat{z}$-direction component of the momentum is transformed.

2.2 Invariant Kinematics

Invariant kinematic variables uniquely describe each event and collectively characterize this experiment. In their most general form these variables are Lorentz invariant. They include the four-momentum transfer squared Q^2, the Bjorken scaling variable x, and the fractional energy z. The distributions of these variables are shown in Figs. 6-11 for the 5.7 GeV two-pion data sample.

The four-momentum of the virtual photon is

$$Q^2 = -q_\mu \cdot q^\mu = -(\nu^2 - \vec{q}^2). \tag{19}$$

When evaluated in the lab frame, where $p \gg m$, this becomes

$$Q^2 = 4kk' \sin^2 \frac{\theta}{2}. \tag{20}$$

The polar angle between k and k', as is used in Eq. 3, is θ. The distribution of Q^2 in Fig. 6 shows most of the events occur between 1-3 GeV.

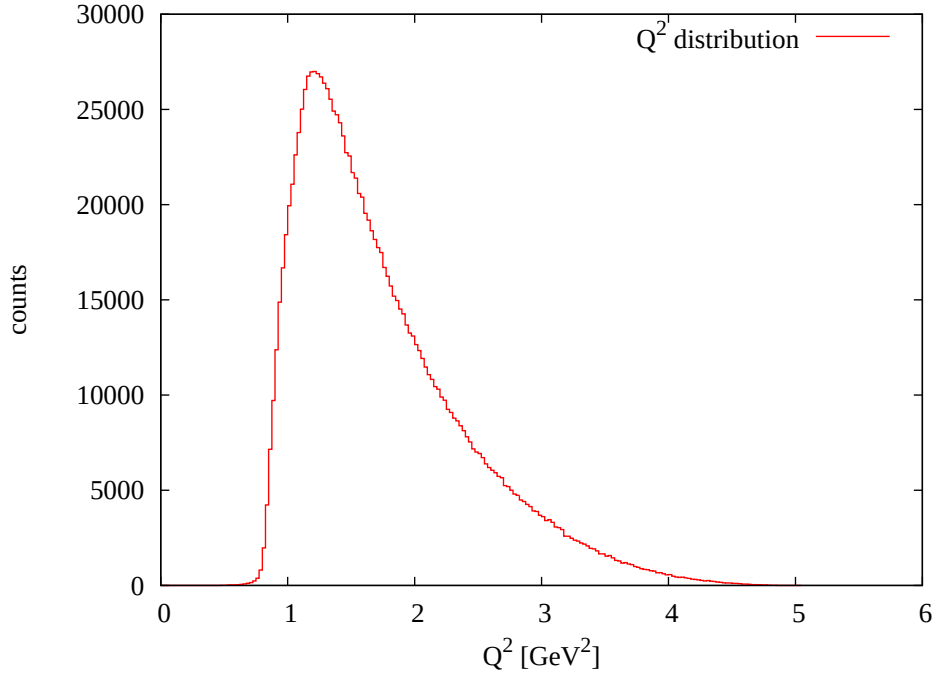

Figure 6: The Q^2 distribution for the 5.7 GeV two-pion data. The average value is 1.75 GeV. The distribution falls off at low Q^2 because the of the acceptance of the CLAS detectors. The distribution falls off at higher Q^2 because the scattering process is less likely.

The Bjorken scaling variable is

$$x = \frac{Q^2}{2M_p\nu}, \tag{21}$$

where M_p is the proton mass. In the limit of large Q^2, x is interpreted as the fraction of momentum of the struck quark compared to the total momentum of the proton. The range of x is between 0 and 1. At $x = 1$, the electron collision is perfectly elastic. In Fig. 7, the x distribution peaks at $x = 0.2$. The detector acceptance limits measuring lower x, while at higher x there is only a small probability of scattering from a quark carrying most of the nucleon's energy.

The fractional energy transfer

$$z = \frac{E_1 + E_2}{\nu}, \tag{22}$$

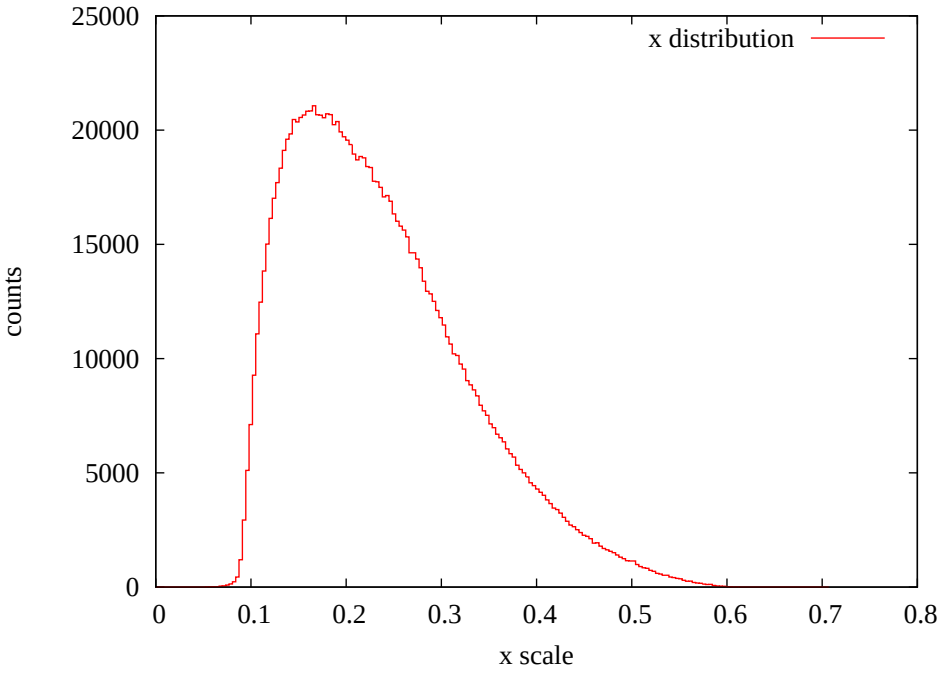

Figure 7: The x distribution for the 5.7 GeV two-pion data. The average value is 0.24.

ranges between 0 and 1 and is the ratio of energy in the pion-pair to the total energy transferred to the nucleon. The histogram of z in Fig. 8 shows a broad distribution that drops off below $z = 0.1$ due to detector acceptance. Although z is defined on the interval $(0, 1)$, a few events are measured with $z > 1$. This is explained by the movement of the proton inside the target nucleus which broadens the distribution beyond $z = 1$.

Figure 9 shows a scatter plot of Q^2 and x. Although, the variables appear to be linearly related, they are independent and are correlated because of detector acceptance. In contrast, the scatter plots of Q^2 vs. z in Fig. 10, and x vs. z in Fig. 11, show no linear dependence.

In four-momentum space the dot product of a four-momentum vector with itself produces an invariant mass quantity. The invariant mass of the virtual photon-nucleon system is

$$W = P_{h\mu} \cdot P_h^{\mu} = \sqrt{2M_p\nu + M_p^2 - Q^2}, \tag{23}$$

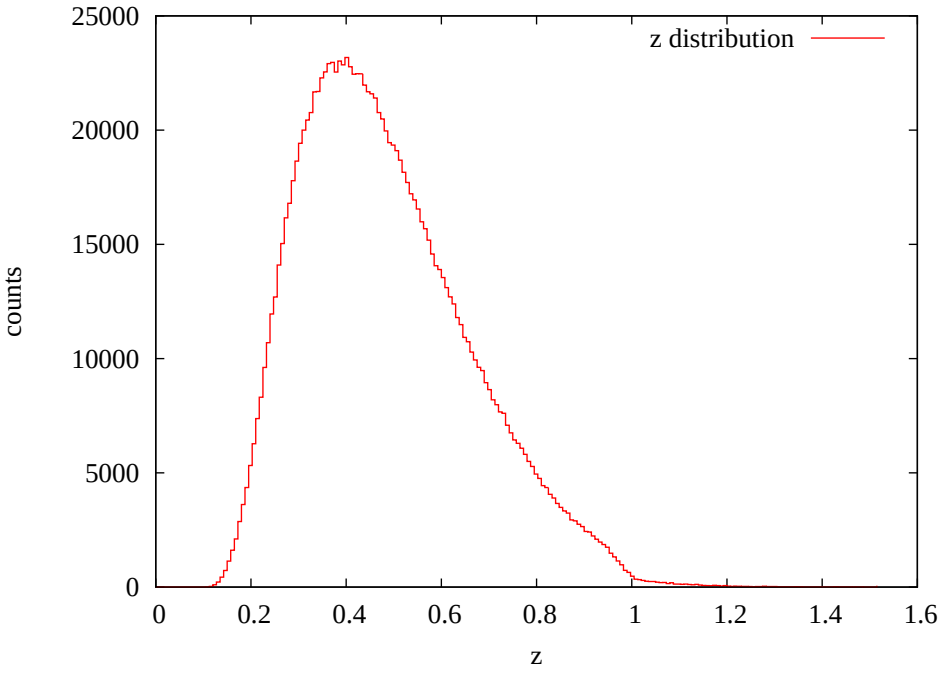

Figure 8: The z distribution for the 5.7 GeV two-pion data. The average value is 0.48. The variable z exceeds 1 here because there is a contribution to the total energy of the ep system from the internal movement of the proton inside the nucleus. When the proton move in the same direction as the virtual photon, the fractional energy can be greater than one.

The invariant mass distribution for this experiment in plotted in Fig. 12. The minimum value occurs at 0.27 GeV which is twice the mass of one pion. The peak at 0.77 GeV, corresponding to the ρ particle which decays into a pion-pair.

3 Calculating the Asymmetry

3.1 Single Spin Asymmetry

A single spin target asymmetry is calculated as a function of the azimuthal angle $\phi_{R\perp}$. Figure 13 depicts an electron scattering from a nucleon for the two possible longitudinally polarized target orientations. The number of expected pion-pair events with a perfectly polarized target for the aligned (or anti-aligned) case is denoted as $n^{\uparrow(\downarrow)}(\phi_{R\perp})$. The ideal asymmetry is given by $A = \frac{n^{\uparrow}(\phi_{R\perp}) - n^{\downarrow}(\phi_{R\perp})}{n^{\uparrow}(\phi_{R\perp}) + n^{\downarrow}(\phi_{R\perp})}$. The observed

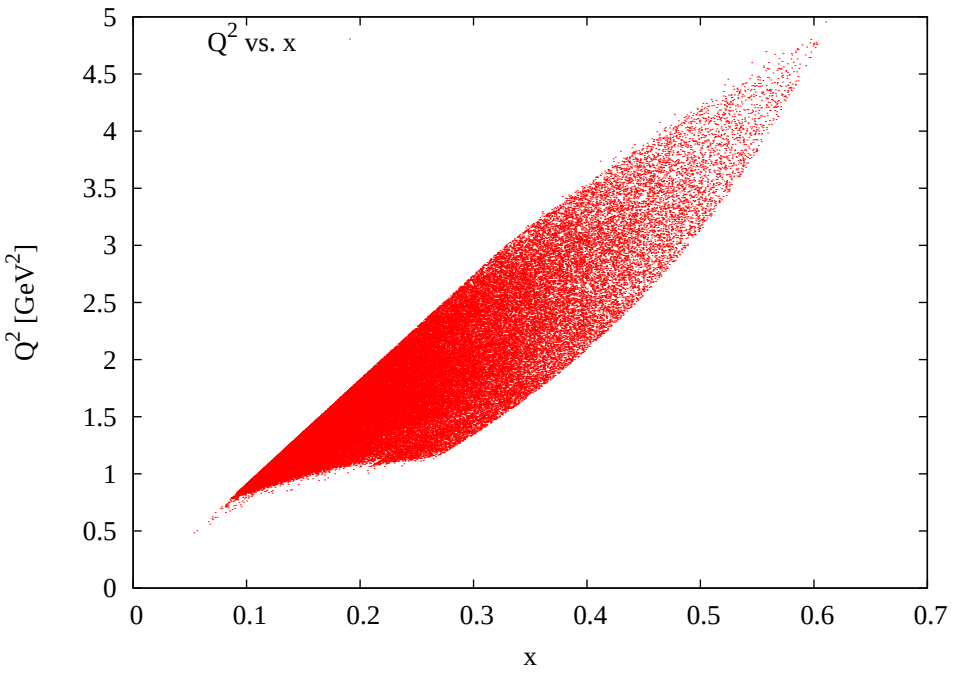

Figure 9: The distribution of Q^2 vs. x for the 5.7 GeV two-pion data. Although x and Q^2 are independent variables, the acceptance of the detector limits the values of Q^2 and x to the region shown. With many other energies and a perfect detector one could populate the entire plot. The plot shows only 25% of the total events recorded in order to more clearly emphasize the density distribution.

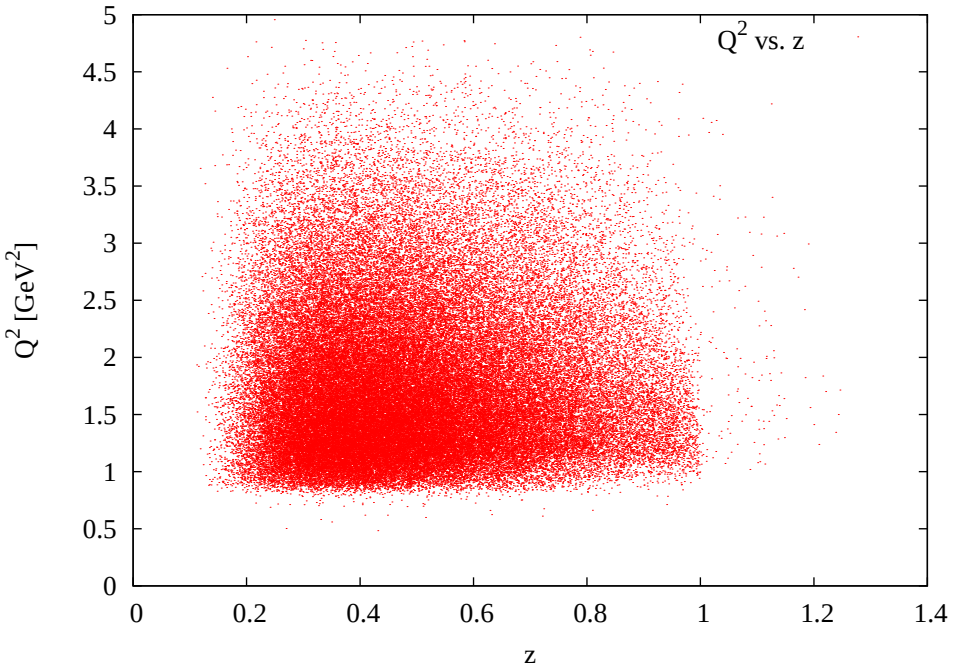

Figure 10: The distribution of Q^2 vs. z for the 5.7 GeV two-pion data. Similarly, for Q^2 and z, the detector limits the ranges of x and Q^2 observed. For $Q^2 < 0.7$ and $z < 0.1$, detector acceptance limits the number of events observed. The plot shows only 25% of the total events recorded.

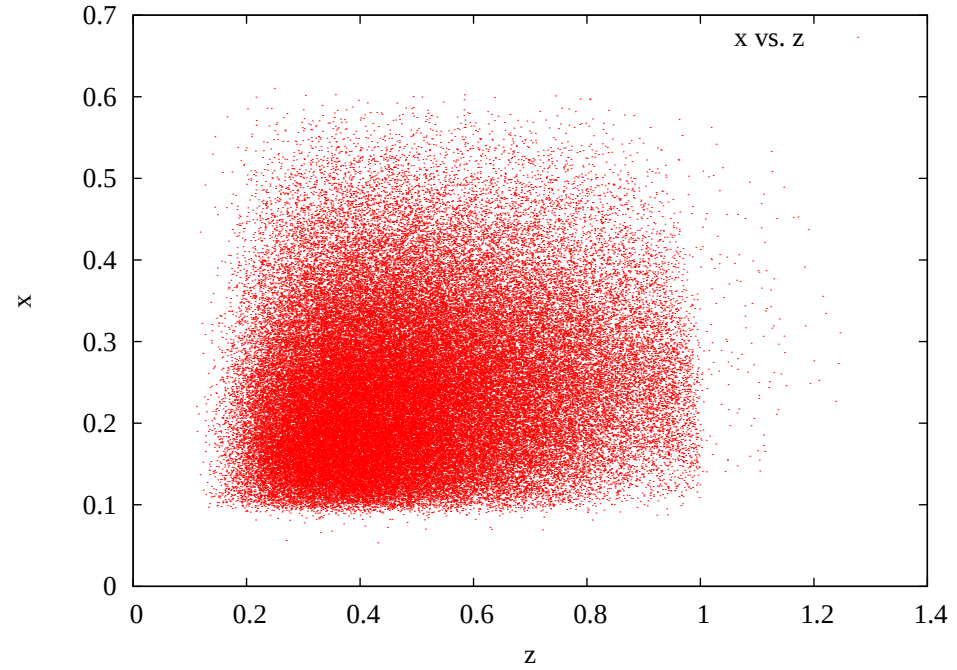

Figure 11: The distribution of x vs. z for the 5.7 GeV two-pion data. The low x and z events are not detected because of the detector acceptance. Above $x = 0.5$ the x distribution falls off. The plot shows only 25% of the total events recorded.

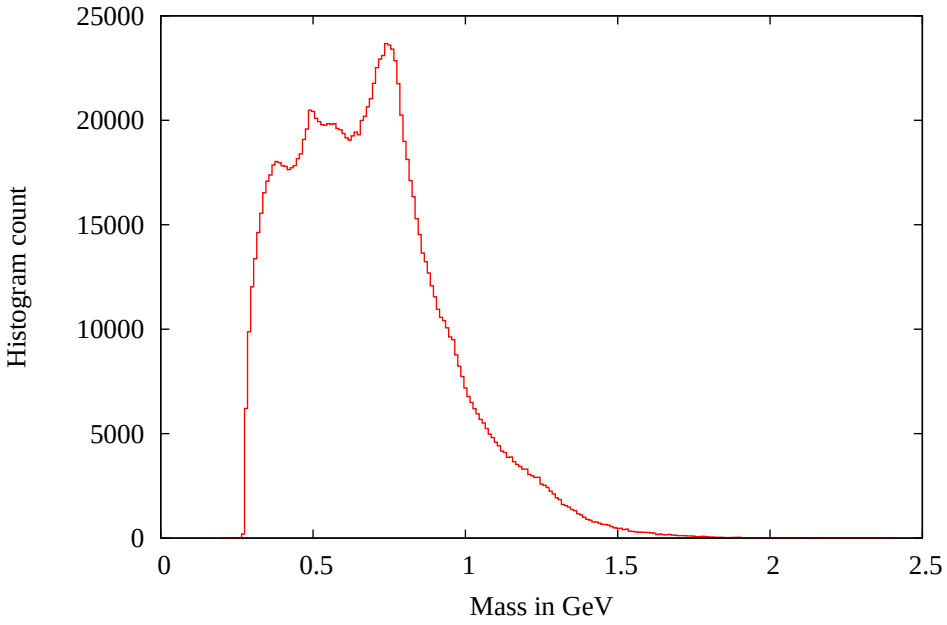

Figure 12: Pion-pair invariant mass. The lower limit $2M_\pi$, the rest mass of the two pions. The range of the invariant mass is 0.27-2.0. The peak at 0.77 GeV, corresponding to the ρ particle which decays into a pion-pair.

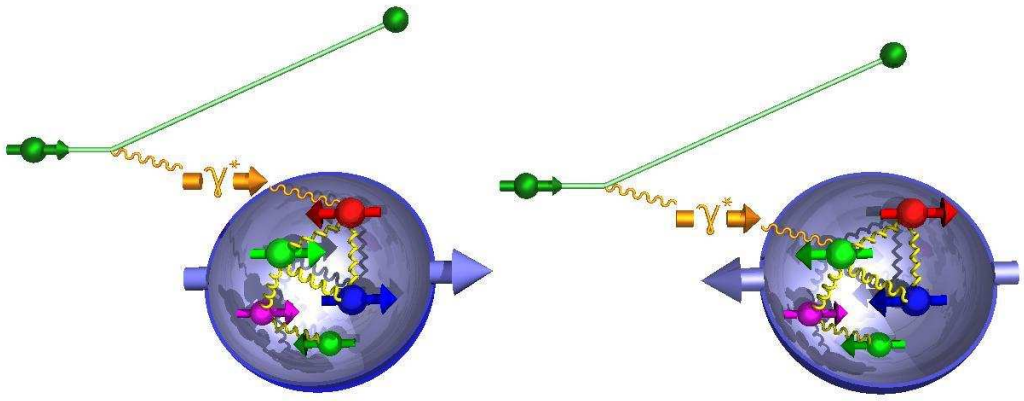

Figure 13: Scattering from a longitudinally polarized target. The left diagram has a proton aligned with the incident electron direction whereas the right diagram has the proton spin anti-aligned with the electron beam [6].

number of events for an aligned (or anti-aligned) polarization is $N^{\uparrow(\downarrow)}(\phi_{R\perp})$. The polarization P, which ranges from (-1, 1) for a given alignment, is related to the probability p of finding a proton with the same alignment by $P^{\uparrow(\downarrow)} = 2p^{\uparrow(\downarrow)} - 1$. The observed number of events are related to the ideal number of events by

$$N^{\uparrow(\downarrow)}(\phi_{R\perp}) = p^{\uparrow(\downarrow)} n^{\uparrow(\downarrow)}(\phi_{R\perp}) + (1 - p^{\uparrow(\downarrow)}) n^{\downarrow(\uparrow)}(\phi_{R\perp}) + n^0(\phi_{R\perp}). \tag{24}$$

Thus, for a polarized sample, the probability of finding the proton with an aligned spin is given by the first term, the probability of finding the proton antialigned is given by the second term, and the third term is the contribution from an unpolarized nucleon. For this experiment, n^0 is the contribution from the mostly unpolarized nitrogen in the ammonia target. Because the nitrogen nucleus is unpolarized, only scattering from the polarized hydrogen atoms should contribute to the asymmetry calculations.

The polarization and counts (the number of $\pi^+\pi^-$ events) in each run are normalized by the beam intensity during that run. To measure beam intensity a Faraday cup collects a charge induced by the electron beam. The weighted polarization, summed over each run i in bins of $\phi_{R\perp}$, is

$$\langle P^{\uparrow(\downarrow)} \rangle = \frac{\sum_i P_i^{\uparrow(\downarrow)} q_i^{\uparrow(\downarrow)}}{\sum_i q_i^{\uparrow(\downarrow)}}, \tag{25}$$

where $q_i^{\uparrow(\downarrow)}$ is the charge collected in that particular run. The normalized number of counts in each bin of $\phi_{R\perp}$ is

$$N^{\uparrow(\downarrow)(\phi_{R\perp})} = \frac{\sum_i N_i^{\uparrow(\downarrow)}(\phi_{R\perp})}{\sum_i q_i^{\uparrow(\downarrow)}}. \tag{26}$$

Therefore, the experimental asymmetry is

$$A_{UL}(\phi_{R\perp}) = \frac{N^{\uparrow}(\phi_{R\perp}) - N^{\downarrow}(\phi_{R\perp})}{\langle P^{\downarrow} \rangle N^{\uparrow}(\phi_{R\perp}) + \langle P^{\uparrow} \rangle N^{\downarrow}(\phi_{R\perp})}, \tag{27}$$

The subscripts L, T, or U represent longitudinal polarization, transverse polarization, or no polarization, respectively. The first index describes the beam polarization followed by the target polarization.

3.2 Theoretical Model

In the theoretical calculations of A. Bacchetta and M. Radici [10], the asymmetry for an unpolarized beam on a transverse target yields,

$$A'_{UT} \sim B(y)\sin(\phi_{R\perp} + \phi_S)h_1 H_1^{\sphericalangle} + (\ldots). \tag{28}$$

Whereas the longitudinal component of the asymmetry is,

$$A'_{UL} = V(y)\sin(\phi_{R\perp})\frac{M}{Q}(h_1 H_1^{\sphericalangle} + g_1\tilde{G}^{\sphericalangle}). \tag{29}$$

The functions $B(y) = 1 - y$ and $V(y) = 2(2-y)\sqrt{1-y}$ depend on the kinematic variable $y = \nu/k$, which is the fraction of energy transfered from the electron into the virtual photon. In a longitudinally polarized target the angle of transverse spin goes to 0, $\phi_S = 0$ in Eq. 28. The functions g_1 and $\tilde{G}^{\sphericalangle}$ are related to the longitudinally polarized quark distribution in the same respect as h_1 and $H_1^{\sphericalangle}$ are related to the transverse distributions. In particular, $h_1(x, Q^2)$ is mainly a function of x and $H_1^{\sphericalangle}(z, Q^2)$ is mainly a function of z. Both functions depend weakly on Q^2. With certain approximations one can measure the transversity functions from Eqs. 28 and 29 by extracting the $\sin\phi_{R\perp}$ moment of the asymmetry A_{UL}.

3.3 Propagation of Error

The asymmetry, $A_{UL}(\phi_{R\perp})$, depends on two variables, $N^{\uparrow}$ and $N^{\downarrow}$, which are taken to be independent. The error on the asymmetry is derived using the standard error propagation formulas and is

$$\delta_A = \sqrt{\left(\frac{\partial A}{\partial N^{\uparrow}}\right)^2 N^{\uparrow} + \left(\frac{\partial A}{\partial N^{\downarrow}}\right)^2 N^{\downarrow}}, \tag{30}$$

where it is assumed $N^{\uparrow}$ and $N^{\downarrow}$ have a Poisson distribution such that $\delta_N = \sqrt{N}$. The partial derivative of A with respect to $N^{\uparrow}$ is

$$\frac{\partial A}{\partial N^{\uparrow}} = \frac{\left(\langle P^{\uparrow}\rangle N^{\downarrow} + \langle P^{\downarrow}\rangle N^{\uparrow}\right) - (N^{\uparrow} - N^{\downarrow})(\langle P^{\downarrow}\rangle)}{(\langle P^{\uparrow}\rangle N^{\downarrow} + \langle P^{\downarrow}\rangle N^{\uparrow})^2}. \tag{31}$$

Simplifying this equation yields

$$\left(\frac{\partial A}{\partial N^{\uparrow}}\right)^2 = \frac{\left(\langle P^{\uparrow}\rangle N^{\downarrow} + \langle P^{\downarrow}\rangle N^{\downarrow}\right)^2}{(\langle P^{\uparrow}\rangle N^{\downarrow} + \langle P^{\downarrow}\rangle N^{\uparrow})^4}. \tag{32}$$

Similarly, the derivative with respect to $N^{\downarrow}$ is

$$\left(\frac{\partial A}{\partial N^{\downarrow}}\right)^2 = \frac{\left(\langle P^{\downarrow}\rangle N^{\uparrow} + \langle P^{\uparrow}\rangle N^{\uparrow}\right)^2}{(\langle P^{\uparrow}\rangle N^{\downarrow} + \langle P^{\downarrow}\rangle N^{\uparrow})^4}. \tag{33}$$

Combining Eqs. 30, 32 and 33 gives the final result for the error

$$\delta_A = \frac{\langle P^{\uparrow}\rangle + \langle P^{\downarrow}\rangle}{(\langle P^{\uparrow}\rangle N^{\downarrow} + \langle P^{\downarrow}\rangle N^{\uparrow})^2}\sqrt{N^{\uparrow}N^{\uparrow}N^{\downarrow} + N^{\uparrow}N^{\downarrow}N^{\downarrow}}. \tag{34}$$

In limit of $\langle P^{\uparrow}\rangle = \langle P^{\downarrow}\rangle = \langle P\rangle$ and $N^{\uparrow} = N^{\downarrow} = N/2$, the error is

$$\delta_A = \frac{1}{\langle P\rangle\sqrt{N}}. \tag{35}$$

This has the expected $1/\sqrt{N}$ of statistical counting error.

4 Experimental Results

The distribution of $A_{UL}(\phi_{R\perp})$ is found by first generating the histograms of $N^{\uparrow}(\phi_{R\perp})$ and $N^{\downarrow}(\phi_{R\perp})$. In Fig. 14, the number of events detected are plotted in bins of $\phi_{R\perp}$. The bimodal structure is a result of the detector acceptance. The target polarized parallel to the electron produces more pion-pairs than the anti-parallel target. The asymmetry, calculated from Eq. 27, is plotted in Fig. 15 with an average value of 0.04

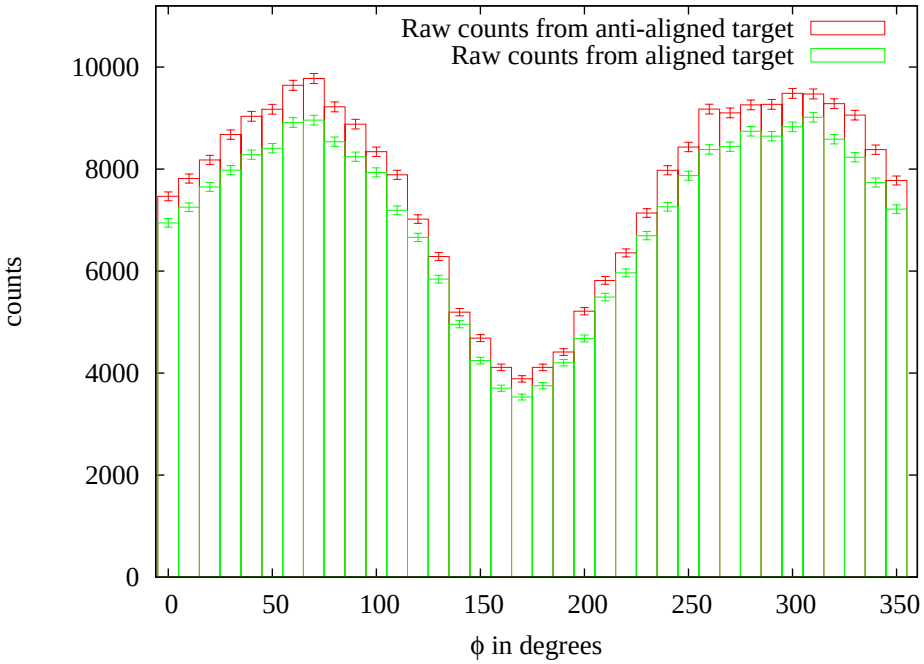

Figure 14: Histogram of raw counts for targets aligned and anti-aligned. The raw counts are from all the runs, but do not include the charge normalization (Eq. 26). The aligned polarization counts (in green) are less than the anti-aligned counts (in red). There are 36 bins of $\phi_{R\perp}$. The distribution dips at 0 and 180 degrees because of detector acceptance.

with large statistical error bars. The asymmetry is fit to a function of $\sin\phi_{R\perp}$ defined by

$$A_{UL}(\phi_{R\perp}) = a_1 + a_2 \sin\phi_{R\perp}, \tag{36}$$

where a_1 and a_2 are the fitting parameters. The coefficient of the $\sin\phi_{R\perp}$ term is defined as

$$a_2 \equiv A_{UL}^{\sin\phi_{R\perp}}. \tag{37}$$

The error bars are the statistical error calculated in Eq. 34. Although the error bars do not conform to the expectations of a statistical distribution, by Eq. 35 and $N \approx 20,000$ the error is expected to be approximately 0.007. This is 17% the value of the magnitude of the asymmetry. Furthermore, the error bars were checked by reducing the data used to calculate the asymmetry to only 1% of the total data and found a 10% increase in the error bar size as expected. This suggests the error bars

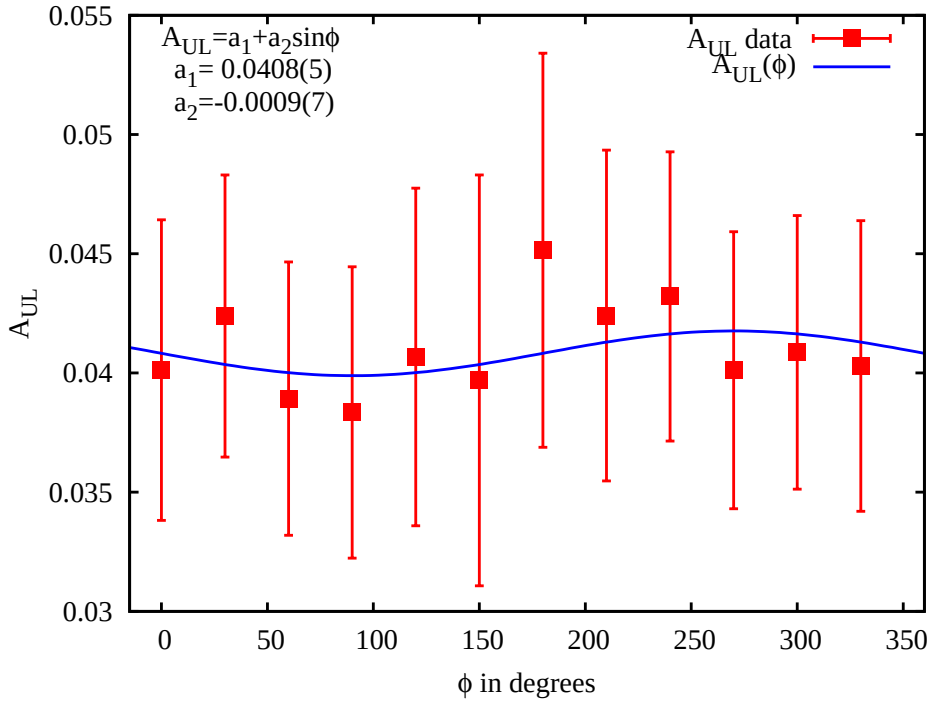

Figure 15: A_{UL} in bins of $\phi_{R\perp}$, fit to a function of $A_{UL} = a_1 + a_2 \sin\phi_{R\perp}$. The overall asymmetry is small with an average value of approximately 0.04. The error bars shown here are statistical.

were calculated correctly.

4.1 Asymmetry over Bins of Q^2, x, and z

The spin structure of the proton at high Q^2 is well known from quantum perturbation theory, but little is known about the accuracy of the approximations at the lower energy limits. The asymmetry is plotted in bins of Q^2, x, and z, and the $\sin\phi_{R\perp}$ moment ($A_{UL}^{\sin\phi_{R\perp}}$) is extracted from each plot. Due to limited statistics, each bin is split only in half according to the median value of the data.

A significant difference is measured in the $\sin\phi_{R\perp}$ moment extracted from two bins of Q^2. Figure 16 shows the lower bin of Q^2 has a significant negative value of $A_{UL}^{\sin\phi_{R\perp}} = -0.0024$. The upper half of the Q^2 bin (Fig. 17) does not have a statistically significant $\sin\phi_{R\perp}$ moment. Similarly, there is a significant difference in the $\sin\phi_{R\perp}$ moment in the two bins of x. The lower bin of x (Fig. 18) has a significant

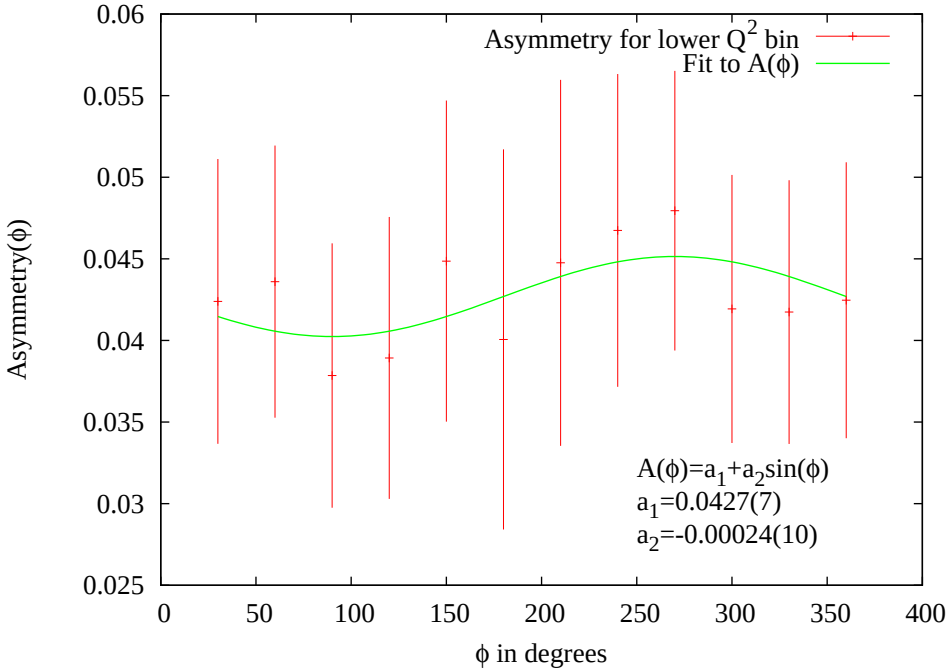

Figure 16: Asymmetry of lower Q^2 bin. A significant $\sin\phi_{R\perp}$ moment can be extracted in this bin of low Q^2.

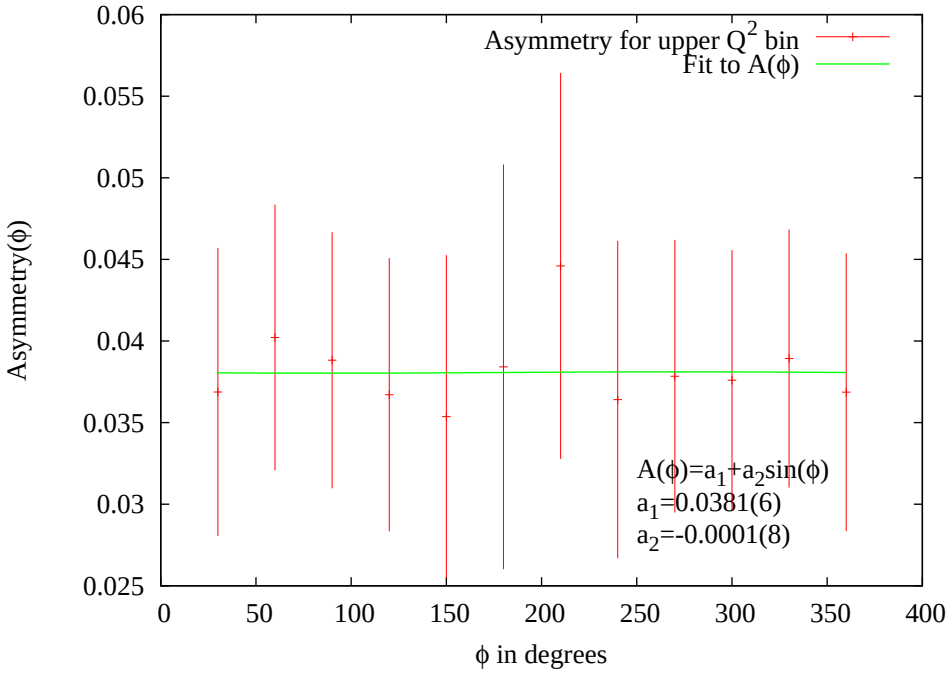

Figure 17: Asymmetry of upper Q^2 bin. There is no statistical $\sin\phi_{R\perp}$ dependence.

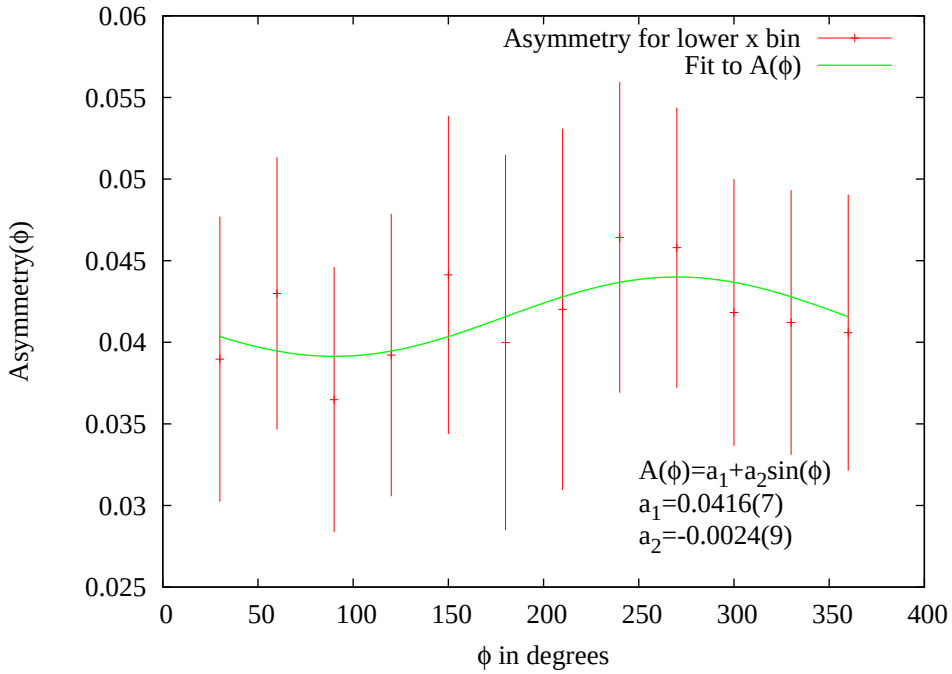

Figure 18: Asymmetry of lower x bin. A significant $\sin\phi_{R\perp}$ moment can be extracted in the lower bin of x of $A_{UL}^{\sin\phi_{R\perp}} = -0.0024$.

negative value of $A_{UL}^{\sin\phi_{R\perp}} = -0.0024$. However, the $\sin\phi_{R\perp}$ moment of the upper bin of x (Fig. 19) is consistent with 0. Lastly, no significant difference exists in the two bins of z. Both Figs. 20 and 21 place a consistent limit on the $\sin\phi_{R\perp}$ moment, $A_{UL}^{\sin\phi_{R\perp}} > -0.002$ and is close to 0. Because of the relatively small value of the measured $\sin\phi_{R\perp}$ moment, the statistical error bars dominate. With more statistics, these measurements will be able to better pin down the value of $A_{UL}^{\sin\phi_{R\perp}}$ and can be compared to other data at higher Q^2 to measure the accuracy of the perturbative method.

The extracted values of $A_{UL}^{\sin\phi_{R\perp}}$ from Figs. 16-21 are plotted in Fig. 22, and the average kinematics of each plot are given in Table 2. The first and third line in the table, corresponding to the upper bins of Q^2 and x respectively, show the most significant non-zero $\sin\phi_{R\perp}$ moment. The statistical values of zero correspond to the highest bins of Q^2 and x (lines 2 and 4, respectively). There only is a small

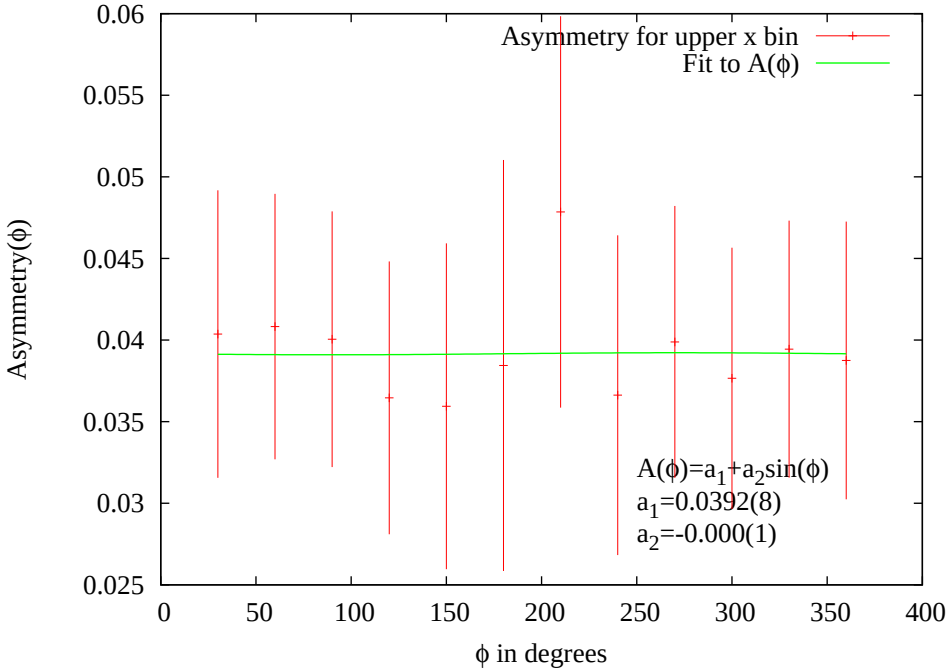

Figure 19: Asymmetry of upper x bin. There is no statistically significant $\sin\phi_{R\perp}$ dependence.

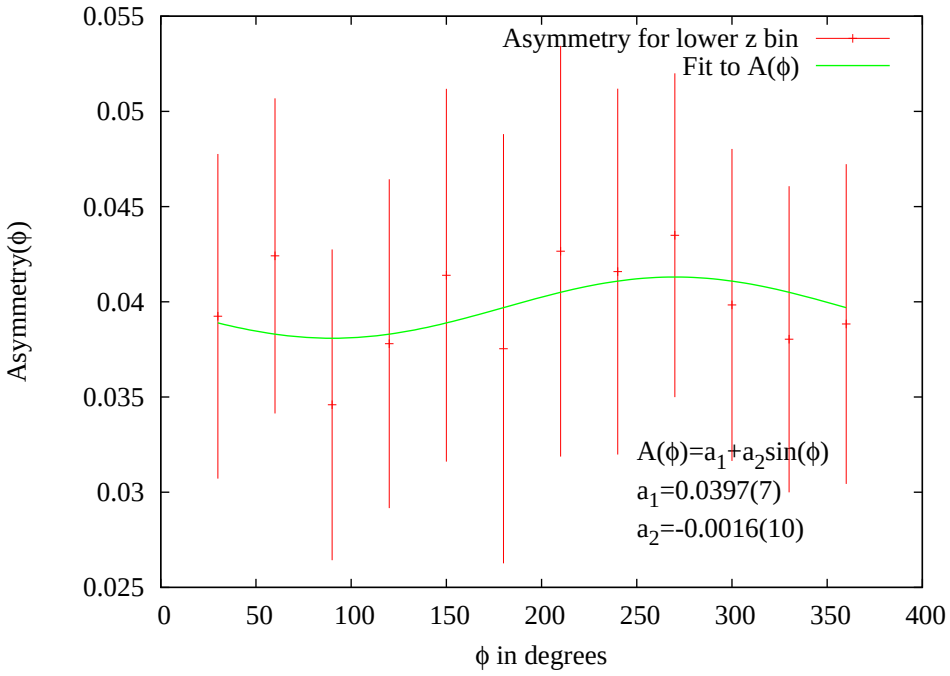

Figure 20: Asymmetry of lower z bin. The asymmetry shows no statistically significant $\sin\phi_{R\perp}$ dependence.

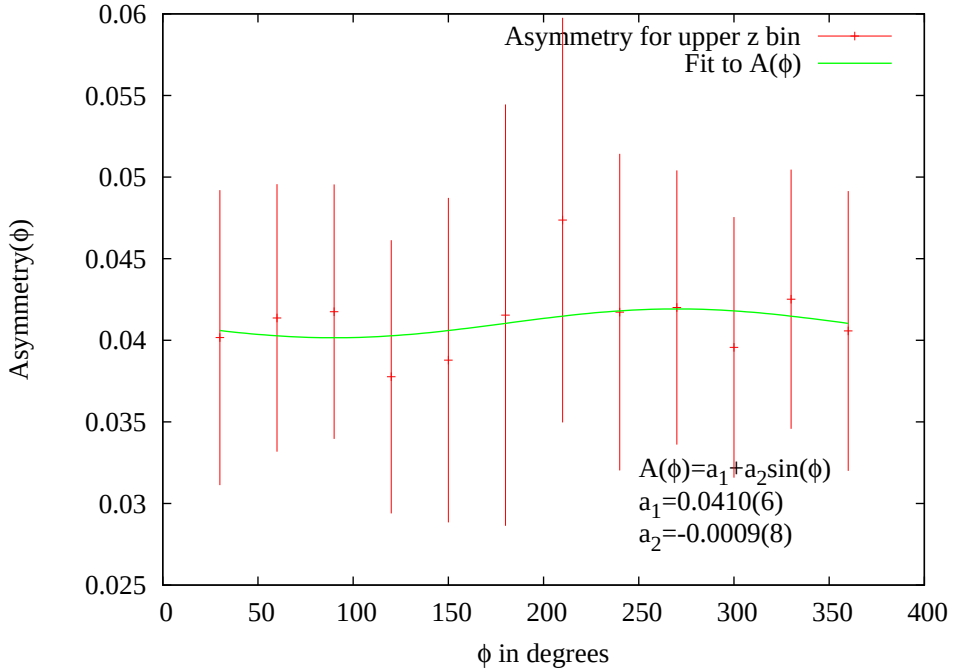

Figure 21: Asymmetry of upper z bin. There is no statistically significant $\sin\phi_{R\perp}$ dependence.

dependence of $A_{UL}^{\sin\phi_{R\perp}}$ on z.

4.2 Dilution Factor

Expanding the asymmetry in Eq. 27 using the definition of the measured counts in Eq. 24, we get

$$A_{UL} = \frac{(p^{\uparrow}n^{\uparrow} + (1-p^{\uparrow})n^{\downarrow}) - (p^{\downarrow}n^{\downarrow} + (1-p^{\downarrow})n^{\uparrow})}{\langle P^{\downarrow}\rangle(p^{\uparrow}n^{\uparrow} + (1-p^{\uparrow})n^{\downarrow} + n^{0}) + \langle P^{\uparrow}\rangle(p^{\downarrow}n^{\downarrow} + (1-p^{\downarrow})n^{\uparrow} + n^{0})}. \tag{38}$$

Q^2 Range (GeV^2)	$\langle Q^2\rangle$ (GeV^2)	x Range	$\langle x\rangle$	z Range	$\langle z\rangle$	$A_{UL}^{\sin\phi_{R\perp}}$
(0.48, 1.57)	1.24	(0.053, 0.33)	0.18	(0.10, 1.46)	0.49	-0.00245(99)
(1.57, 4.96)	2.24	(0.17, 0.61)	0.31	(0.11, 1.27)	0.50	-0.00004(82)
(0.48, 2.07)	1.29	(0.053, 0.23)	0.17	(0.10, 1.32)	0.47	-0.00243(94)
(0.98, 4.96)	2.19	(0.23, 0.61)	0.32	(0.11, 1.46)	0.52	-0.00006(105)
(0.48, 4.96)	1.72	(0.053, 0.61)	0.23	(0.10, 0.47)	0.35	-0.00161(98)
(0.54, 4.90)	1.76	(0.059, 0.61)	0.25	(0.47, 1.46)	0.65	-0.00088(78)

Table 2: Averages of kinematics plotted in Figs. 16-21. The bins were distributed equally, split above and below the median. Statistical differences in Q^2 and x bins can be seen in the corresponding figures. Figure 22 plots the $A_{UL}^{\sin\phi_{R\perp}}$ dependence of each bin.

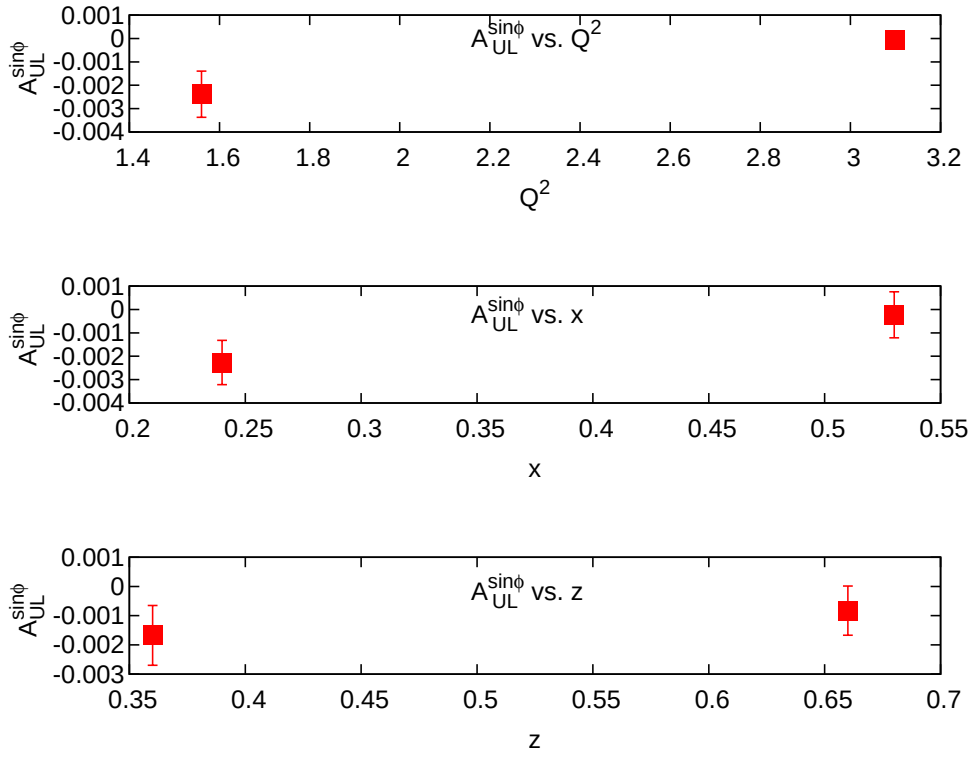

Figure 22: Plots of $A_{UL}^{\sin\phi_{R\perp}}$ vs. Q^2, x, and z. The lower Q^2 and x bins have a value that is statistically less than zero, while both higher bins of higher Q^2 and x have an answer that is statistically 0. The bins of of z show a $\sin\phi_{R\perp}$ moment less than zero, but the values do not significantly change.

Because pion production will be the same for two unpolarized nitrogen nuclei (under equal conditions), the n^0 term in the numerator cancels. To account for such terms in the denominator a dilution factor f is introduced such that it scales the experimental asymmetry to extract the actual asymmetry, or

$$\frac{n^\uparrow - n^\downarrow}{n^\uparrow + n^\downarrow} = \frac{1}{f}\left(\frac{N^\uparrow - N^\downarrow}{\langle P^\downarrow\rangle N^\uparrow + \langle P^\uparrow\rangle N^\downarrow}\right). \tag{39}$$

Using Eq. 39, f is rewritten in terms of $n^\uparrow$, $n^\downarrow$, and n^0 as

$$f = \frac{n^\uparrow + n^\downarrow}{n^\uparrow - n^\downarrow}\left(\frac{N^\uparrow - N^\downarrow}{\langle P^\downarrow\rangle N^\uparrow - \langle P^\uparrow\rangle N^\downarrow}\right). \tag{40}$$

By expanding P and N according to their definitions in terms of p and n, this is

$$f = \frac{n^\uparrow + n^\downarrow}{n^\uparrow - n^\downarrow}\left(\frac{(n^\uparrow - n^\downarrow)(p^\uparrow + p^\downarrow - 1)}{(n^\uparrow + n^\downarrow + 2n^0)(p^\uparrow + p^\downarrow - 1)}\right). \tag{41}$$

Finally, this yields the result

$$f = \frac{n^\uparrow + n^\downarrow}{n^\uparrow + n^\downarrow + 2n^0}. \tag{42}$$

This is the fraction of the contribution of events from hydrogen over the total contribution of ammonia. The expected value is approximately 3/18, the ratio of nucleons in the three hydrogen atoms over the total ammonia atom.

4.2.1 Missing Mass

This semi-inclusive experiment measures only the electron and two pions in the final state. The missing mass is defined as the mass difference between the four-momenta of the virtual photon and proton and the four-momenta of the two pions. The missing mass in this experiment is

$$MM^2 = \left(P_\mu + q_\mu - P_{1\mu} - P_{2\mu}\right)^2, \tag{43}$$

where P_μ is the four-momenta of the proton. In its rest frame the proton has a four-momenta of $P_\mu = (M_p, \vec{0})$.

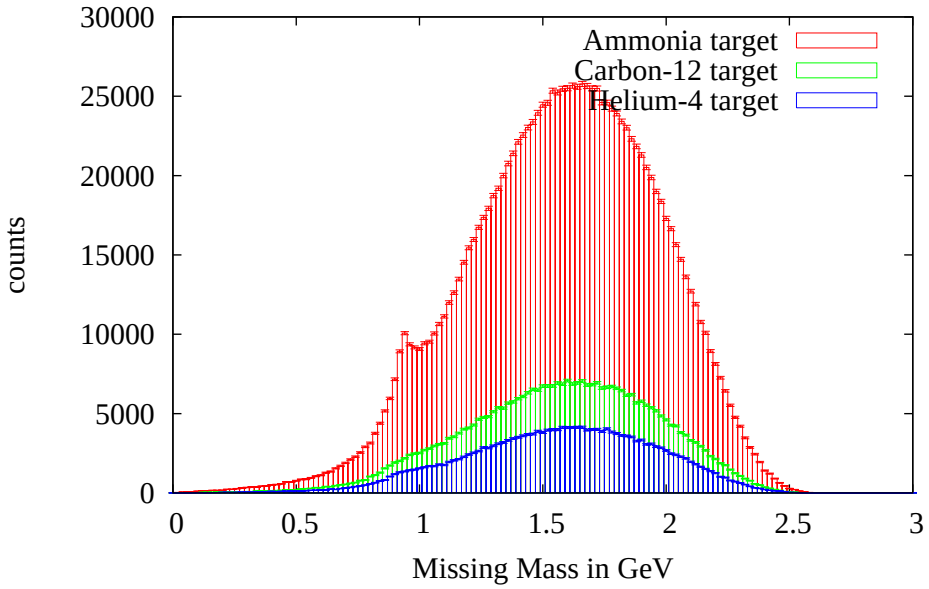

Figure 23: Missing mass spectrum for NH_3, ^{12}C, and ^4He targets. Conservation of baryon number, charge, etc, requires at minimum a nucleon in the scattering equation. The peak at 0.93 GeV is the mass of nucleon. Above is a large distribution of other combination of particles.

When only two pions are produced and detected, the missing mass is that of a single nucleon. Figure 23 shows the distribution of missing mass and at 0.9 GeV, the mass of a nucleon, there is a small peak for the ammonia target. The measurements below 0.9 GeV are due to the Fermi motion of the nucleons inside the nucleus. Measurements above the 0.9 GeV peak result from events that produce more than one nucleon and two pions in the final state.

Measuring the dilution factor requires extracting the hydrogen events from the ammonia events. The dilution factor is equivalent to the scattering cross section of the polarized protons in hydrogen over the total ammonia cross section. This is given by

$$f = \frac{\sigma_{H_3}}{\sigma_{^{15}NH_3}}. \tag{44}$$

Measuring the proton events with a pure nitrogen (^{15}N) target would simply require subtracting the nitrogen events from the ammonia events. Instead the carbon (^{12}C)

target that is used must be scaled such that the 12 carbon nucleons resemble nitrogen's 15 nucleons. The scaling ratio is determined by $r_f = \sigma_{^{15}NH_3}/\sigma_{^{12}C}$, but in a kinematic region where the hydrogen protons in ammonia do not contribute to the number of events measured. Rewriting the dilution factor to reflect the data from this experiment gives

$$f = \frac{\sigma_{^{15}NH_3} - \sigma_{^{15}N}}{\sigma_{^{15}NH_3}} = \frac{\sigma_{^{15}NH_3} - r_f\sigma_{^{12}C}}{\sigma_{^{15}NH_3}}. \tag{45}$$

Quantum mechanical conservation laws require that during the $\pi^+\pi^-$ production at least one other particle remains. The smallest remnant is the nucleon from which the electron was scattered. The events counted below the nucleon mass are a result of Fermi motion of the nucleons in a large atomic nucleus. Therefore, only nitrogen can contribute in this region. Finding a value for r_f requires that only data below the 0.9 GeV peak be used. The 0.9 GeV peak is fit to a Gaussian curve to find its center. Using only the data three standard deviations below the center removes 99.7% of the events that originated from the polarized proton. Figure 24 shows a scaling ratio of $r_f = 3.18$ between nitrogen and carbon in the missing mass range of 0.48 to 0.87 GeV. In this range, there are good statistics that are below the range of proton events.

Using the scaling factor r_f, we scale the carbon nucleus to resemble the nitrogen nucleus and calculate the dilution factor using Eq. 45. The scaled ^{12}C target is compared with the ^{15}N target in Fig. 25. The plot shows the events from the carbon target closely mimic the events from nitrogen below nucleon peak. The peak is more distinct in the ammonia target. The difference between the ammonia events and scaled carbon events are the hydrogen proton events.

The dilution factor measured as a function of missing mass is found by taking the ratio of the number of proton events to the number of ammonia events. The dilution factor is shown in Fig. 26 where the nucleon missing mass peak is still clear. Below the peak, the dilution factor is statistically consistent with zero, while above the peak

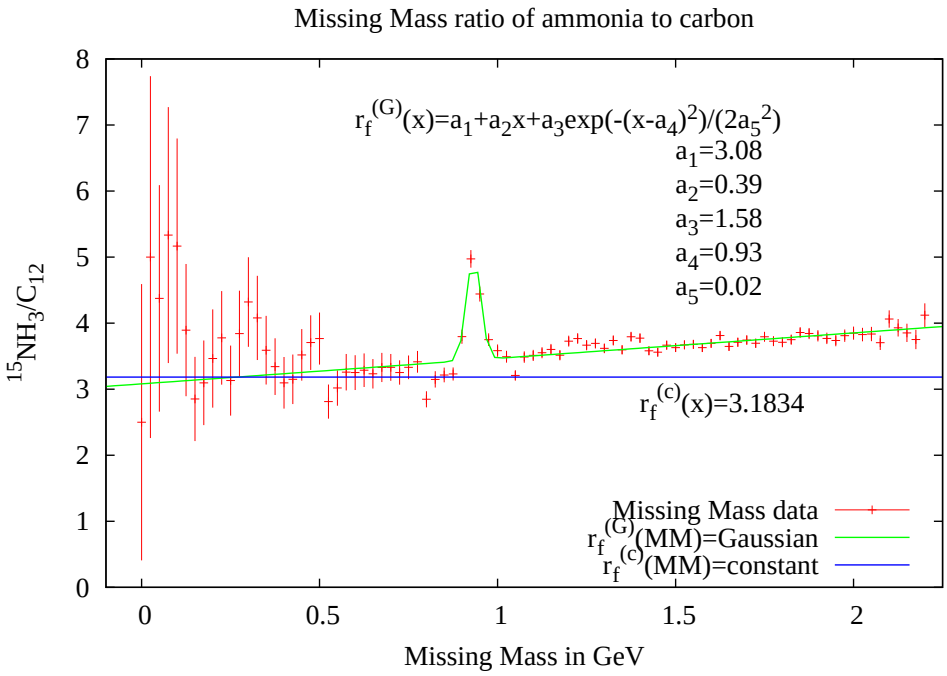

Figure 24: Missing mass distribution of $^{15}NH_3/^{12}C$ The number of counts from the ammonia target divided by the counts from the carbon target is plotted as a function of missing mass. At 0.9 GeV, the missing mass is equal to a nucleon. The distribution below this peak is attributed to Fermi motion of the nitrogen nucleus. To find the ratio of events, only three standard deviations below from the Gaussian peak are used to find r_f. For $0.48 < MM < 0.8735$ a ratio is of $r_f = 3.1835$ is measured. This value is used to scale the ^{12}C data to resemble the ^{15}N nucleus.

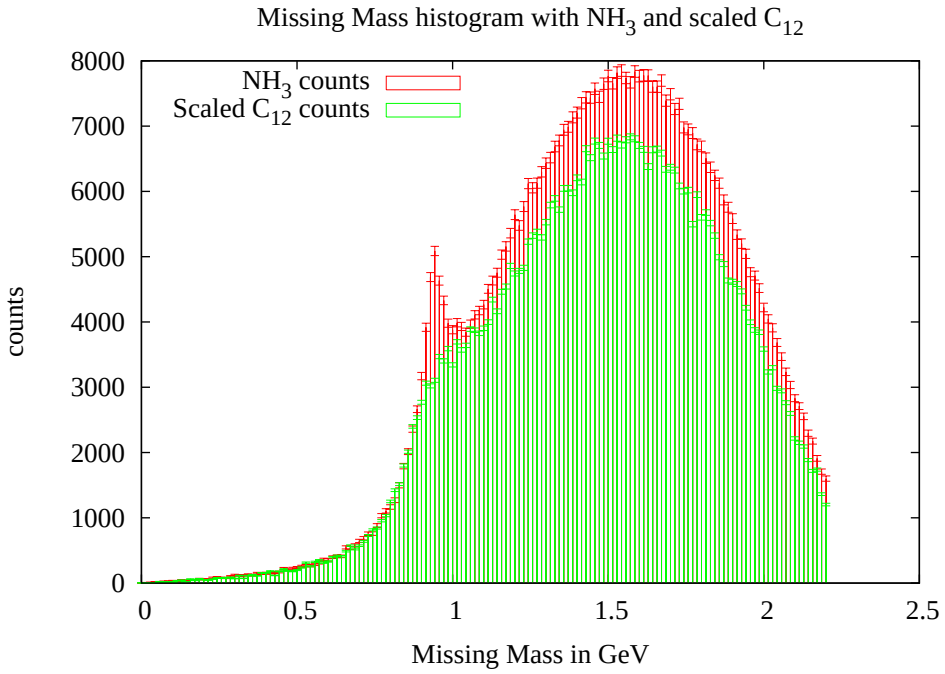

Figure 25: Comparison of missing mass histogram of $^{15}NH_3$ and C_{12} scaled to mimic ^{15}N. As found in Fig. 24, ^{12}C is scaled by 3.1835 to get the ^{15}N contribution. As expected, below 0.9 GeV the carbon events closely resemble nitrogen events. The different of the two histograms are the events that originate from proton events.

it has an average value of $f = 0.14$. This is less than a one percent error from the expected value of 3/18.

Finally, the dilution factor is plotted as a function of $\phi_{R\perp}$. The number of the events from the ammonia and carbon targets are counted and the dilution factor is calculated using Eq. 45. As shown in Fig. 27, the dilution factor has a small $\cos\phi_{R\perp}$ dependence, but is otherwise relatively constant with $f = 0.13$, and is consistent with the dilution factor of $f = 0.14$ in Fig. 26.

4.2.2 The Asymmetry with the Dilution Factor

The final asymmetry, which includes the dilution factor scaling, shows the best estimate for the $\sin\phi_{R\perp}$ moment for $A_{UL}(\phi_{R\perp})$. The moment is given by $A_{UL}^{\sin\phi_{R\perp}} = -0.018(9)$. The asymmetry data in Fig. 28 is scaled by the dilution factor, $1/f$, from

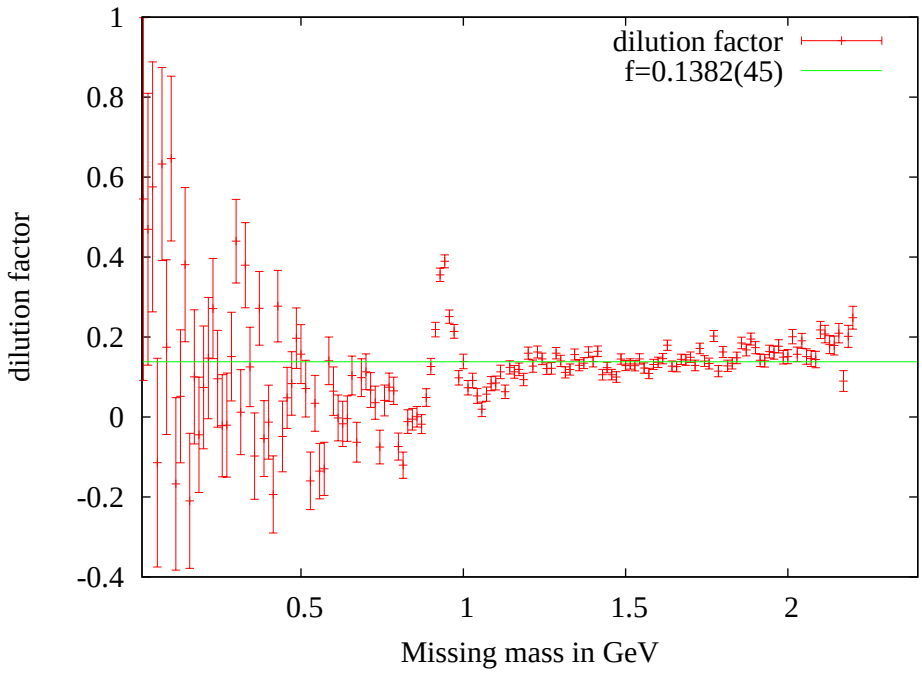

Figure 26: Dilution factor vs. missing mass. The peak from missing mass of only a nucleon at 0.9 GeV is still present. Below the peak the dilution factor is statistically 0 and above the peak $f = 0.138$. The constant $f = 0.138$ is plotted in green and is less than one percent error from the predicted dilution factor of 3/18.

Fig. 27. The error on the dilution factor is taken to be a systematic error. Other systematic errors are not included because the statistical errors are much larger than the systematic errors in this experiment.

5 Conclusions

From a single spin asymmetry of $\pi^+\pi^-$ production, a measurement is made on quark transversity in a proton. The $\sin\phi_{R\perp}$ moment of the asymmetry places a limit on the transversity distribution and fragmentation function $h_1(x, Q^2)H_1^{\sphericalangle}(z, Q^2)$. For the kinematics $\langle Q^2\rangle = 1.75$, $\langle x\rangle = 0.23$, and $\langle z\rangle = 0.50$, we measured the moment to be $A_{UL}^{\sin\phi_{R\perp}} = -0.0065 \pm 0.005(stat)$. This is a first measurement of the JLab data on the for 2-pion production as a measure of transversity.

It would be interesting to compare this data with an experiment after JLab up-

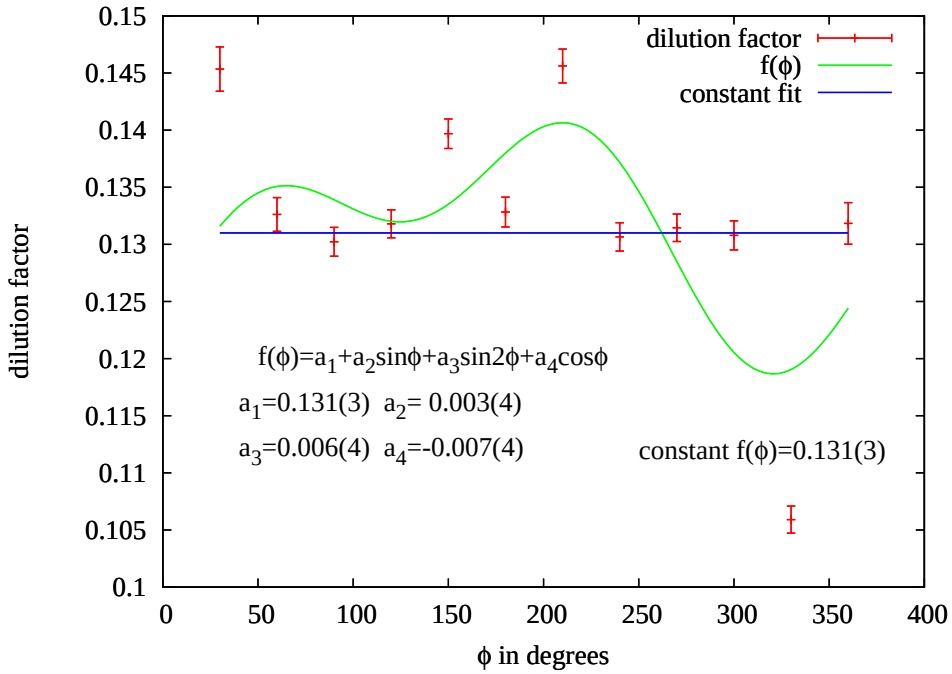

Figure 27: Dilution factor vs. ϕ for all $W < 2.2$. The constant $f(\phi_{R\perp}) = 0.13$ (in blue) is consistent with the fit in Fig. 26. This value is slightly lower because the missing mass below 0.9 GeV was included. The sinusoidal fit (in green) shows no statistically significant $\sin\phi_{R\perp}$ dependence, but there is a small negative $\cos\phi_{R\perp}$ and a small positive $\sin\phi_{R\perp}$ dependence.

grades to higher energy. The test of perturbative quantum dynamics and the search for the origin of proton spin makes this an exciting future experiment to be further studied.

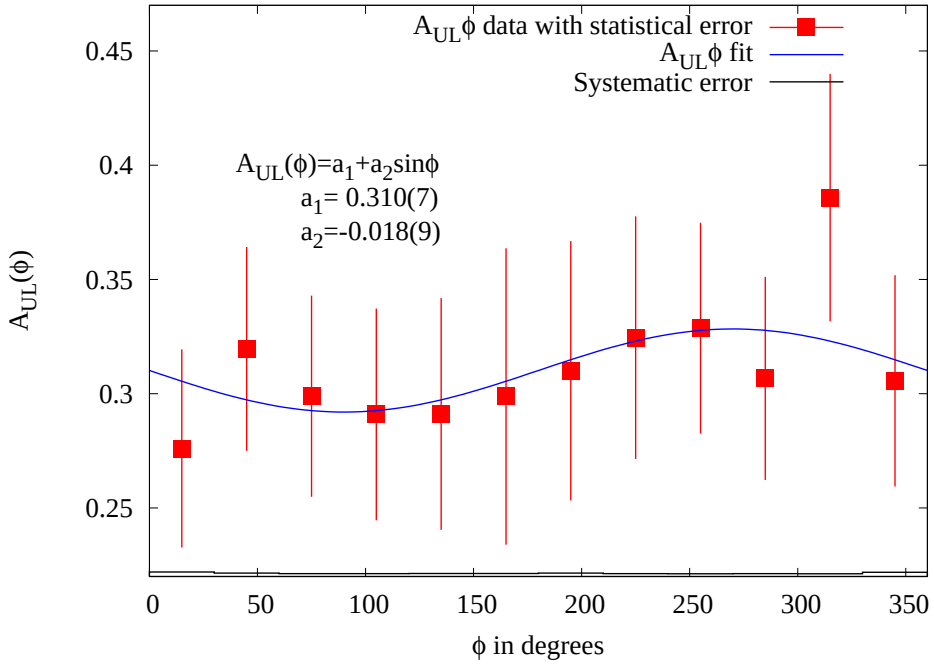

Figure 28: Final $A_{UL}(\phi_{R\perp})$ with statistical and systematic errors. Taking the asymmetry from Fig. 15 and scaling by the dilution factor in Fig. 27 the asymmetry is calculated as $A_{UL}(\phi_{R\perp}) = 0.31 - 0.02 \sin\phi_{R\perp}$. The statistical error bars are included in the data, while the magnitude of the dilution factor error is plotted along the bottom of the graph and has an average value of 0.13.

References

[1] J. Ashman *et al.*, Phys. Lett. B **206**, 1 (1988).

[2] P. L. Antony *et al.*, Phys. Lett. B **458**, 529 (1999).

[3] K. Abe *et al.*, Phys. Rev. Lett. **79**, 26 (1997).

[4] V. Barone, A. Drago, and P. G. Ratcliffe, Phys. Rept. **359**, 1 (2002), hep-ph/0104283.

[5] M. Radici, R. Jakob, and A. Bianconi, Phys. Rev. D **65**, 074031 (2002).

[6] U. Elschenbroich, Images available from HERMES at DESY, <`http://www-hermes.desy.de/notes/pub/trans-public-subject.html`> [Accessed 11 April 2007].

[7] S. Kuhn, EG1 Collaboration at Jefferson Lab, 2000, <`http://jlab.org/~kuhn/EG2000intro.html`> [Accessed: 22 April 2007].

[8] B. A. Mecking *et al.*, Nucl. Instr. Meth. in Phys. Res. A **503**, 513 (2003).

[9] A. Bacchetta, U. D'Alesio, M. Diehl, and C. A. Miller, Phys. Rev. D **70**, 117504 (2004).

[10] A. Bacchetta and M. Radici, (2004), hep-ph/0407345.

A Code–fileprint.pl

The following Perl code calculates the general kinematics for each event. It requires the run information and the twopi file from the experiment.

```
#!/usr/bin/perl -w

#-------------------------------------------
# INPUT FILES
#    runinfo.txt
#         includes target polarization,
#         beam energy, and charge collected
#         for each run)
#    r#####.twopi
#         for each run a unique file with
#         beam polarization, momentum of
#         the scattered electron, and both
#         pion momentum.
#
# OUTPUT to <STOUT>
#-------------------------------------------
use Math::Trig;
use diagnostics;

#Define masses of particles in GeV
$MEL = 0.000510999;#electron
$MP = 0.93827;     #proton
$MPI = 0.13957;    #pion

$count=0;
$runnum = 27070;   #first runnum of data

open(FH, "< ./runinfo.txt") or
                die "couldn't open file $!";
@ARRAY = <FH>;     #holds information from runinfo
close(FH);

$p_count=0;
$targ_n_acc=0;
$n_count=0;
$targ_p_acc=0;

$ebeam=5.736;      #beam energy,GeV

while ($runnum < 27500) { #end of run files
  if (-e "r$runnum.twopi") { #if file exists
    open DATA, "< r$runnum.twopi" or
                print "couldn't open file:$!";
    #DATA contains file r#####.twopi

    while (<DATA>) #reads each line in DATA
```

```
{
  @array = split;
  $count++;
  #$polarization = $array[0];
  $pion1 = $array[1]; #pion1 charge
  $pion2 = $array[2]; #pion2 charge
  $elx = $array[3];   #electron mometum
  $ely = $array[4];   #in cartesian coords
  $elz = $array[5];   #in units of GeV
  #make the leading pion with + charge
  if ($pion2==1 && $pion1==-1) {
    $pi2x = $array[6];
    $pi2y = $array[7];
    $pi2z = $array[8];
    $pi1x = $array[9];
    $pi1y = $array[10];
    $pi1z = $array[11];
    $cont=1;
  }
  elsif($pion1==1 && $pion2==-1) {
    $pi1x = $array[6];
    $pi1y = $array[7];
    $pi1z = $array[8];
    $pi2x = $array[9];
    $pi2y = $array[10];
    $pi2z = $array[11];

    $kprime = sqrt($MEL*$MEL+$elx*$elx+$ely*$ely+$elz*$elz);
    #conservation of momentum from electron to q
    if ($runnum > 27300) {$ebeam=5.628;} #beam energy changes
    #beam comes in z direction with momentum = beam energy
    $qx = -$elx;
    $qy = -$ely;
    $qz = $ebeam-$elz;
    $nu = $ebeam-$kprime; #energy of q
    #e^2=m^2+p^2 for pion energy calculation
    $pi1E = sqrt($MPI*$MPI+$pi1x*$pi1x+$pi1y*$pi1y+$pi1z*$pi1z);
    $pi2E = sqrt($MPI*$MPI+$pi2x*$pi2x+$pi2y*$pi2y+$pi2z*$pi2z);

    ###MASS invariant (sum sq)
    $Esum = $pi1E+$pi2E;
    ##########################
    ### pi PAIR ###############
    @PPh = (($pi1x+$pi2x), ($pi1y+$pi2y), ($pi1z+$pi2z));
    @PPhabs = (abs($PPh[0]), abs($PPh[1]), abs($PPh[2]));
    $PPhmag = sqrt($PPh[0]*$PPh[0]+$PPh[1]*
     $PPh[1]+$PPh[2]*$PPh[2]);
    @PPhat = ($PPh[0]/$PPhmag, $PPh[1]/$PPhmag, $PPh[2]/$PPhmag);
    $Epairhat = $Esum/$PPhmag;
    $pisum= sqrt (FOUR($Esum, @PPh));
    #invariant mass from sum of pions
    #gamma when pi pair is in rest frame
```

```
$gamma = $Esum / ($pisum);

#########################################################
#              pi transform                             #
#########################################################

$pi1para= ($pi1x*$PPhat[0]+$pi1y*$PPhat[1]+$pi1z*$PPhat[2]);
@pi1perp= ( $pi1x-(($pi1para)*$PPhat[0]),$pi1y-(($pi1para)*
          $PPhat[1]), $pi1z-(($pi1para)*$PPhat[2]));

$pi2para=($pi2x*$PPhat[0]+$pi2y*$PPhat[1]+$pi2z*$PPhat[2]);
@pi2perp=($pi2x-(($pi2para)*$PPhat[0]),$pi2y-(($pi2para)*
        $PPhat[1]),$pi2z-(($pi2para)*$PPhat[2]));

#lorentz transform
@pi1paratransform= LORENTZ ( $gamma, $pi1E, $pi1para);
@pi2paratransform= LORENTZ ( $gamma, $pi2E, $pi2para);
@pi1tvect= ( $pi1paratransform[1]*$PPhat[0],
             $pi1paratransform[1]*$PPhat[1],
             $pi1paratransform[1]*$PPhat[2]);
@pi2tvect= ( $pi2paratransform[1]*$PPhat[0],
           $pi2paratransform[1]*$PPhat[1],
           $pi2paratransform[1]*$PPhat[2]);
@pi1tT= ( ($pi1tvect[0])+$pi1perp[0],
           ($pi1tvect[1])+$pi1perp[1],(
            $pi1tvect[2])+$pi1perp[2] );
$pi1tmagT= sqrt(DOT(@pi1tT, @pi1tT));
$pi1tT[2]/$pi1tmagT);
#theta CM
$theta1piT = acos ($pi1paratransform[1]/$pi1tmagT);

@pi2tT= ( $pi2tvect[0]+$pi2perp[0],
           $pi2tvect[1]+$pi2perp[1],
           $pi2tvect[2]+$pi2perp[2] );
$pi2tmagT= sqrt(DOT(@pi2tT, @pi2tT));
#@pi2that = ($pi2tT[0]/$pi2tmag, $pi2tT[1]/$pi2tmag,
          $pi2tT[2]/$pi2tmag);
$theta2piT = acos ($pi2paratransform[1]/$pi2tmagT);

@pairtest= LORENTZ ( $gamma, $Esum, $PPhmag);
print ("pairtest\t $pairtest[0] $pairtest[1]\n");

#check lorentz by unboosting back to lab frame
@pi1labagain=( $pi1perp[0]+$pi1tvect[0],
               $pi1perp[1]+$pi1tvect[1],
               $pi1perp[2]+$pi1tvect[2] );
@pi2labagain=( $pi2perp[0]+$pi2tvect[0],
               $pi2perp[1]+$pi2tvect[1],
               $pi2perp[2]+$pi2tvect[2]);
print ("checklabframe @pi1labagain\n");
print ("checklabfram2 @pi2labagain\n");
```

```
######################
# ANGLES IN PION PAIR #
######################
@qcrossk = ($qy*$elz - $ely*$qz, $qz*$elx-$elz*$qx,
            $qx*$ely-$elx*$qy);
#RR
@RR = ( ($pi1x-$pi2x)/2, ($pi1y-$pi2y)/2, ($pi1z-$pi2z)/2 );
$Ediff = ($pi1E-$pi2E)/2;
print ("RR(diff/2)\t $Ediff @RR\n");
@RRabs = ( abs($RR[0]), abs($RR[1]), abs($RR[2]) );
#@RRmag = sqrt($RR[0]*$RR[0]+$RR[1]*$RR[1]+$RR[2]*$RR[2]);

#theta specific
$RdotPPhat = ($RR[0]*$PPhat[0]+$RR[1]*$PPhat[1]+
              $RR[2]*$PPhat[2]);
@RT = ($RR[0]-($RdotPPhat)*$PPhat[0],
       $RR[1]-($RdotPPhat)*$PPhat[1],
       $RR[2]-($RdotPPhat)*$PPhat[2]);
print ("R_t @RT\n");
$RdotPPh = ($RR[0]*$PPh[0]+$RR[1]*$PPh[1]+$RR[2]*$PPh[2]);
$RabsdotPPhabs = ($RRabs[0]*$PPhabs[0]+$RRabs[1]*$PPhabs[1]+
                  $RRabs[2]*$PPhabs[2]);
$theta = acos ($RdotPPh/ $RabsdotPPhabs);

#phi
$qcrosskdotRT = ($qcrossk[0]*$RT[0]+$qcrossk[1]*$RT[1]+
                 $qcrossk[2]*$RT[2]);
@qcrossRT = ($qy*$RT[2]-$qz*$RT[1], $qz*$RT[0]-$qx*$RT[2],
             $qx*$RT[1]-$qy*$RT[0]);
$qcrosskdotqcrossRT = ($qcrossk[0]*$qcrossRT[0]+
                       $qcrossk[1]*$qcrossRT[1]+
                       $qcrossk[2]*$qcrossRT[2]);
@qcrosskabs = (abs($qy*$elz - $ely*$qz),
               abs($qz*$elx-$elz*$qx),
               abs($qx*$ely-$elx*$qy));
$qcrosskmag = sqrt(DOT(@qcrossk, @qcrossk));
@qcrossRTabs = (abs($qy*$RT[2]-$qz*$RT[1]),
                abs($qz*$RT[0]-$qx*$RT[2]),
                abs($qx*$RT[1]-$qy*$RT[0]));
$qcrossRTmag = sqrt(DOT(@qcrossRT, @qcrossRT));
$qcrosskdotqcrossRTabs = ($qcrosskabs[0]*$qcrossRTabs[0]+
                          $qcrosskabs[1]*$qcrossRTabs[1]+
                          $qcrosskabs[2]*$qcrossRTabs[2]);
$multiplymag = $qcrosskmag*$qcrossRTmag;
$sign = ($qcrosskdotRT );
if ($sign > 0) {
 $phirperp =  acos ($qcrosskdotqcrossRT / $multiplymag );
 }
else {
 $phirperp = - acos ($qcrosskdotqcrossRT / $multiplymag );
 }
```

```
printf ("theta-and-phi_r_perp: %.9f %.5f\n",
  $theta, $phirperp);
$phidegree = 180*$phirperp/3.14159265;
printf ("phirperp_degrees: %.9f\n", $phidegree);

#  KINEMATIC INVARIANTS
#  Q^2, x, W, nu, Z
$q2 = -$nu*$nu + $qx*$qx + $qy*$qy + $qz*$qz;
if ($nu eq 0) {print "nu\n"; exit 0;}
else {$xx=$q2/(2*$MP*$nu);}
$ww = sqrt($MP*$MP + 2*$MP*$nu - $q2);
$nu = $ebeam - $kprime;
$zz = $Esum / $nu;
printf ("q2,x,w,zz,phi: %.5f %.5f %.5f %.5f\n\n",
                      $q2, $xx, $ww, $zz, $phidegree);

#calculate INVARIANT of a four vector
#$kinv = FOUR ($kprime, $elx, $ely, $elz);
$invcart = FOUR ($nu, $qx, $qy, $qz);
$mmass=sqrt ( FOUR( $nu+$MP-$Esum,
                    $qx-$PPh[0], $qy-$PPh[0], $qz-$PPh[2]));

 if ($mmass < 2.2) {
  #print data
  printf ("pi1 pi2 %i %i\n", $pion1, $pion2);
  printf ("k\'4(k\',pe):\t %.5f   %.5f   %.5f   %.5f\n",
                    $kprime, $elx, $ely, $elz);
  printf ("q4(nu,q):\t %.5f   %.5f   %.5f   %.5f\n",
                    $nu, $qx, $qy, $qz);
  printf ("pi1four(piE,ppi) %.5f   %.5f   %.5f   %.5f\n",
                    $pi1E, $pi1x, $pi1y, $pi1z);
  printf ("pi2four\t\t %.5f   %.5f   %.5f   %.5f\n",
                    $pi2E, $pi2x, $pi2y, $pi2z);
  print ("pi1Lor\t\t $pi1paratransform[0] @pi1tT\n");
  print ("pi2Lor\t\t $pi2paratransform[0] @pi2tT\n");
  print ("theta12\t\t $theta1piT $theta2piT\n");
  print ("pi1mag\t\t $pi1tmagT\n");
  printf ("inv_mass:\t %.5f\n", $pisum);
  print ("ppairhat\t $Epairhat @PPhat\n");
  print ("pipair\t\t $Esum @PPh\n");
  print ("pairtest\t $pairtest[0] $pairtest[1]\n");
  print ("checklabframe @pi1labagain\n");
  print ("checklabfram2 @pi2labagain\n");
  print ("RR(diff/2)\t $Ediff @RR\n");
  print ("R_t\t\t @RT\n");
  printf ("q2,x,w,zz,phi:\t %.5f   %.5f   %.5f   %.5f\n",
                    $q2, $xx, $ww, $zz, $phidegree);
  printf ("theta-and-phi_r_perp:  %.9f  %.5f\n",
                    $theta, $phirperp);
  printf ("phirperp_degrees: %.9f\n", $phidegree);
   print ("q2_x_z_teta_phi_thecm: $q2 $xx $zz
           $theta $phirperp $theta1piT\n");
```

```
        } #end if missing mass below
      }### end if pi+ pi- pair
    }#end while
    close DATA;
  }#end if runnum exists
  $runnum++;
}#end while run through all data


##########  subroutines
sub FOUR {
  #input (e,p_x,p_y,p_z)
  $invariant = $_[0]*$_[0]-$_[1]*$_[1]-$_[2]*$_[2]-$_[3]*$_[3];
  return $invariant ;
}

sub DOT {
  #input (x1,y1,z1,x2,y2,z2)
  $dotvalue = ( $_[0]*$_[3]+$_[1]*$_[4]+$_[2]*$_[5]);
  return $dotvalue;
}

sub LORENTZ {
  #input (beta or gamma, energy, p_z)
  if (1.0 > $_[0]) {
    $beta = $_[0];
    $gamma = 1/sqrt(1-$beta*$beta ) ;
  }
  else {
    $gamma = $_[0];
    $beta = sqrt(1-(1/($gamma*$gamma)));
  }
  @lorentzarray = (($gamma*($_[1]-$beta*$_[2])),
                   ($gamma*($_[2]-$beta*$_[1])));
  #array output (energy, momentum z)
  return @lorentzarray
}
```

B Code–runPolNH3.pl

The Perl program runPolNH3.pl is a sample code that bins measurements for the asymmetry in bins of ϕ. Using in conjunction with the code in Appendix C.

```
#!/usr/bin/perl -w
#---------------------------------
# Output: phicountX.hist
#
# This program is designed to read
# in data from the two-pion experi-
# ment and analyze the asymmetries
```

```
# and the polarizations involved.
# for Polarized NH3 runs in 6 GeV.
#--------------------------------
use Math::Trig;
use diagnostics;

#histogram info
my (@Ncountpos,@Ncountneg,@ppave,@pnave,@chargesumplus,
@chargesumminus,@ppbinave,@pnbinave);

$bins=12.0;                    #number of bins
#initializes array for counting histogram
for ($ii=0; $ii < $bins; $ii++) {
  $Ncountpos[$ii]=0;
  $Ncountneg[$ii]=0;
  $ppave[$ii]=0;
  $pnave[$ii]=0;
  $chargesumplus[$ii]=0;
  $chargesumminus[$ii]=0;
  }
$division=0;                   #minimum bin
$maximum=360;                  #maximum bin

#Set constants
$MEL = 0.000510999;#MASS of electron, GeV
$MP = 0.93827;#MASS of proton, GeV
$MPI = 0.13957;#MASS of pion, GeV
$count=0;

$totalevents=0;
$PI=3.14159265;

#editted start runnum to keep N+=N-
$runnum = 27078;#from r#####.twopi


#beam energy,GeV
$ebeam=5.736;

while ($runnum < 27500) {
  if (-e "r$runnum.twopi") {
    open(FH, "< ../twopions/runinfo.txt") or die "couldn't open file $!";
    @ARRAY = <FH>;
    close (FH);

    @line=grep(/^\s*$runnum/, @ARRAY);
    if (@line) {
      (@vv)=split(/\s+/,$line[0]);
      if ($vv[7]) {
        if ($vv[7] ne "NH3") {;}#print ("$runnum $vv[7]\n");}
        else {
          $count=0;
```

```
  #print ("run $runnum\n");
  $totalevents+=$vv[8];
  open DATA, "< r$runnum.twopi"
   or print "couldn't open twopi : $!";
while (<DATA>)
{
  @array = split;
  $count++;
  #$polarization = $array[0];#use for the n counts
  $pion1 = $array[1];
  $pion2 = $array[2];
  $elx = $array[3];
  $ely = $array[4];
  $elz = $array[5];
  #puts positive pion first in calculations
  if ($pion2==1 && $pion1 == -1) {
    $pi2x = $array[6];
    $pi2y = $array[7];
    $pi2z = $array[8];
    $pi1x = $array[9];
    $pi1y = $array[10];
    $pi1z = $array[11];
    $pionpair=1;
  }
  elsif ($pion1==1 && $pion2 == -1) {
    $pi1x = $array[6];
    $pi1y = $array[7];
    $pi1z = $array[8];
    $pi2x = $array[9];
    $pi2y = $array[10];
    $pi2z = $array[11];
    $pionpair=1;
  }
  else { $pionpair=0;}
  if ($pionpair == 1) {#run the analysis
    $kprime = sqrt($MEL*$MEL+$elx*$elx+$ely*$ely+$elz*$elz);
    $qx = -$elx;
    $qy = -$ely;
    if($runnum > 27200){$ebeam=5.628;}
    $qz = $ebeam-$elz;
    $nu = $ebeam-$kprime;
    $pi1E = sqrt($MPI*$MPI+$pi1x*$pi1x+$pi1y*$pi1y+$pi1z*$pi1z);
    $pi2E = sqrt($MPI*$MPI+$pi2x*$pi2x+$pi2y*$pi2y+$pi2z*$pi2z);
    $Esum = $pi1E+$pi2E;

    @PPh = (($pi1x+$pi2x), ($pi1y+$pi2y), ($pi1z+$pi2z));
    $PPhmag = sqrt($PPh[0]*$PPh[0]+$PPh[1]*$PPh[1]+
              $PPh[2]*$PPh[2]);
    @PPhat = ($PPh[0]/$PPhmag, $PPh[1]/$PPhmag,
              $PPh[2]/$PPhmag);
    @qcrossk = ($qy*$elz - $ely*$qz, $qz*$elx-$elz*$qx,
                $qx*$ely-$elx*$qy);
```

```
@RR = ( ($pi1x-$pi2x)/2, ($pi1y-$pi2y)/2,
      ($pi1z-$pi2z)/2 );
$RdotPPhat = ($RR[0]*$PPhat[0] + $RR[1]*$PPhat[1]
              + $RR[2]*$PPhat[2]);
@RT = ($RR[0] - ($RdotPPhat)*$PPhat[0],
 $RR[1]-($RdotPPhat)*$PPhat[1],
 $RR[2]-($RdotPPhat)*$PPhat[2]);

#phi
$qcrosskdotRT = ($qcrossk[0]*$RT[0] + $qcrossk[1]*$RT[1] +
                 $qcrossk[2]*$RT[2]);
@qcrossRT = ($qy*$RT[2]-$qz*$RT[1], $qz*$RT[0]-$qx*$RT[2],
              $qx*$RT[1]-$qy*$RT[0]);
$qcrosskdotqcrossRT = ($qcrossk[0]*$qcrossRT[0]+$qcrossk[1]*
                    $qcrossRT[1]+$qcrossk[2]*$qcrossRT[2]);
$qcrosskmag = sqrt(DOT(@qcrossk, @qcrossk));
$qcrossRTmag = sqrt(DOT(@qcrossRT, @qcrossRT));
$multiplymag = $qcrosskmag*$qcrossRTmag;
$sign = ($qcrosskdotRT );
#phi
if ($sign > 0) {
  $phi_r_perp =  acos ($qcrosskdotqcrossRT /
   $multiplymag );}
else {
  $phi_r_perp = 2*$PI - acos ($qcrosskdotqcrossRT /
   $multiplymag );}
#convert phi to degree's
$phirp_degree = $phi_r_perp * 180 / $PI;

#missing mass
$MMfour=FOUR($nu+$MP-$Esum, $qx-$PPh[0], $qy-$PPh[1],
 $qz-$PPh[2]);
if ( $MMfour >= 0.0 && $MMfour <= 4.84 )
{ ##CUT AT 2.2 GeV in histogram
  $datatrue=1;
}
else {$datatrue=0;}
if  ($datatrue==1){
  ########################## histogram sort
  $division=0; #resets division each new variable
  for ($jj=0; $jj < $bins; $jj++) {
    $divminimum=$division;#set lower bin
    $division += ($maximum / $bins); #sets upper bin
    if ($phirp_degree < $division  &&
     $phirp_degree >= $divminimum) {
      if ($datatrue==1) {
      #target is positive or negative: count respectively
        if ($vv[5] > 0) {
          $Ncountpos[$jj]+=1/$vv[9];
          $ppave[$jj] += $vv[5]*$vv[9]/10000;
          $chargesumplus[$jj] += $vv[9]/100;
        }
```

```
                    elsif ($vv[5] < 0) {
                      $Ncountneg[$jj]+=$vv[9];
                      $pnave[$jj] += $vv[5]*$vv[9]/10000;
                      $chargesumminus[$jj] += $vv[9]/100;
                    }
                  }#if datatrue
                }#if in phi bin
              }#end for loop
              ########################## end histogram sort
              }
            }#if pionpair is plus/minus
          }#while
          close DATA;


        }#else (i.e. a NH3)
        @vv= (0,0);
      }#if target is in array
    }#if line in runinfo
  }#if twopi exists
  $runnum++;
}#while in folder for beam energy

##############################
#  histogram print out
$hcount=0;
open HIST, "> phicountNH3.hist" or
print "cannot print histogram count:$!";
  foreach $ele (@Ncountpos) {
    $histc=$hcount*360/$bins;
    $ppbinave=$ppave[$hcount]/$chargesumplus[$hcount];
    $pnbinave=-$pnave[$hcount]/$chargesumminus[$hcount];
    print HIST "$histc $Ncountpos[$hcount] $Ncountneg[$hcount]
     $ppbinave $pnbinave $chargesumplus[$hcount]
     $chargesumminus[$hcount] $beamppos[$hcount]
     $beampneg[$hcount] $beamnpos[$hcount]
     $beamnneg[$hcount]\n";
    $hcount++;
  }
close HIST;

########  subroutines
sub DOT {
  $dotvalue = ( $_[0]*$_[3]+$_[1]*$_[4]+$_[2]*$_[5]);
  return $dotvalue;
}

sub FOUR {
  $invariant = $_[0]*$_[0] - $_[1]*$_[1] - $_[2]*$_[2] - $_[3]*$_[3];
  return $invariant ;
}
```

C Code–Asym.pl

Here is a sample Perl code that calculates the asymmetry from the output of the program in Appendix B.

```
#!/usr/bin/perl -w
#---------------------------------
# input   ./phicountNH3.hist
#
# output  <STOUT>
#
# this program computes the asymmetry
# from two histograms, one from positive
# target polarization the other negative
# target polarization
#---------------------------------

# input format:
#Nbin   [0-350] [N+] [N-] [P+] [P-] [q+] [q-]
#$bin   [0]     [1]  [2]  [3]  [4]  [5]  [6]
# where,
#N+ = sum( N+_bin ) counts for a polarization in a bin of phi
#P+ = sum( P+_bin * e+_bin) polarization in a bin of phi
#e+ = sum( e+_bin ) charge collected in a bin of phi

open FILE, "< ./phicountNH3.hist" or die "could not open file $!";
@bin=<FILE>;
close FILE;

$count=0;
foreach (@bin) {$count++;} #count number of bins in file
$i=0;
foreach (@bin)
{
    @dat=split(/\s/,$bin[$i]);
    $ppave=$dat[3];
    $pnave=$dat[4];
    $Npnorm=$dat[1] / $dat[5];
    $Nnnorm=$dat[2] / $dat[6];

    $top=$Npnorm-$Nnnorm;
    $bottom=($ppave*$Nnnorm)+($pnave*$Npnorm);
    $asymmetry=$top/$bottom;
    $sqroot=sqrt(($dat[1]*$dat[2]*$dat[2])+
                ($dat[1]*$dat[1]*$dat[2]));
    $bot2=$bottom*$bottom;

    $delta_a=$dat[5]*$dat[6]*($dat[4]+$dat[3])*sqroot/$bot2;

    #divide output into same number of bins as input
    $spacing=360/$count;
```

```
    #print out phi in degrees (0-360)
    $twopirad= $spacing*$i;

    printf ("$twopirad $asymmetry $delta_a\n");
    $i++;
}
```